

sci. Reps. 22:297–308.
osomes for pulmonary
arm. Sci. 14:37–46.
spin resonance, electron

MINI REVIEW

Towards an Understanding of Complex Biological Membranes from Atomistic Molecular Dynamics Simulations

Leonor Saiz,^{1,3} Sanjoy Bandyopadhyay², and Michael L. Klein¹

Received November 26, 2001

Computer simulation has emerged as a powerful tool for studying the structural and functional properties of complex biological membranes. In the last few years, the use of recently developed simulation methodologies and current generation force fields has permitted novel applications of molecular dynamics simulations, which have enhanced our understanding of the different physical processes governing biomembrane structure and dynamics. This review focuses on frontier areas of research with important biomedical applications. We have paid special attention to polyunsaturated lipids, membrane proteins and ion channels, surfactant additives in membranes, and lipid-DNA gene transfer complexes.

KEY WORDS: Biomembranes; membrane proteins; lipid-DNA complexes; lipid-protein interactions; gene therapy; polyunsaturated lipids; surfactants; nicotinic acetylcholine receptor ion channel; peptide bundle; docosahexaenoic fatty acid; fluid lamellar phase.

INTRODUCTION

Biological membranes are sheetlike assemblies of amphipathic molecules that separate cells from their environment and form the boundaries of the different organelles inside the cells [1]. These physical barriers, however, allow a controlled interplay and exchange of material amongst the different parts of the cell and with the external world. Membrane structure and function is accomplished by a complex composition. Biomembranes are, thus, composed of a mixture of lipids, proteins, and carbohydrates. Lipids, in particular, constitute their main component and structural basis. The diversity existent in the lipid composition of cell membranes is a fundamental ingredient. For instance, since cells are usually constrained to an environment where temperature and pressure are fixed, membrane properties can be controlled by varying its composition (lipid type and cholesterol content, for example).

Lipid molecules are also interesting at the fundamental level. These amphiphilic molecules in water display a rich variety of mesophases, which are controlled mainly by temperature and lipid/water composition [1, 2]. Among these structures, the disordered fluid lamellar phase, L_{α} , is the most relevant in biology. Due to the complexity inherent in the biologically relevant systems, theoreticians, computer

¹Center for Molecular Modeling and Chemistry Department, University of Pennsylvania, 231 S. 34th St., Philadelphia, PA 19104-6323.

²Department of Chemistry, Indian Institute of Technology, Kharagpur 721 302, West Bengal, India

³To whom correspondence should be addressed. E-mail: leonor@cmm.chem.upenn.edu

simulators, and experimentalists have adopted simplified models to aid them to understand the main properties of more complex membranes [1–3]. Pure lipid bilayers in the fluid lamellar phase represent the simplest of these biomembrane models.

Computer simulations provide a unique tool to analyze membrane properties from an atomic perspective and offer a direct connection between the microscopic details of the system and the macroscopic properties of experimental interest [4, 5]. Recent developments in the field of computer simulations of model biomembranes [5] have improved our understanding of the physical mechanisms governing their structure and dynamics. In particular, classical molecular dynamics (MD) simulation studies have been extensively used in the last decade to investigate pure lipid bilayer models [6–14]. Due to the excellent agreement with experiment, computer simulations are being used to probe more complex systems with potential biomedical applications (see, for instance, Refs. [15–19] for recent reviews and references therein). This complexity is achieved by introducing multiple components, such as small amphipathic molecules or other solutes, membrane peptides or proteins, or other biopolymers, into a simple model lipid bilayer. The level of detail available from atomic based computer simulations offers unique possibilities not only for the interpretation of experimental data but also to generate novel insights into crucial issues in membrane biophysics.

In this article, we focus on important complex (multicomponent) membranes from frontier areas of biomedical research. In particular, we consider subjects as diverse as highly unsaturated lipids, membrane peptides and ion channels, surfactant additives in membranes, and lipid–DNA gene transfer complexes. To illustrate each of these topics, we present four examples, which constitute the most recent developments in the field. Specifically, we will discuss the effect of highly polyunsaturated mixed-chain lipids on the membrane biophysical properties, the effect of surfactants on biomembranes, transmembrane proteins functioning as ion channels and their effect of the lipid environment, and the nature of lipid–DNA interactions in the lipid–DNA complexes that may be relevant in gene therapy.

METHODS: MD SIMULATIONS

Classical molecular dynamics simulations consist of the integration of the equations of motion for a many-body system of interacting particles [4, 5]. This method can provide direct information on the structure and dynamics of complex biological systems and a detailed picture of atomic and molecular motions subject to the limitations of classical mechanics and knowledge of the intermolecular interaction potentials (force fields). To handle the latter, effective pair potentials are commonly used, where the many-body interactions are reduced to the computation of interactions between pairs of molecules. Usually, they can be described as nonpolarizable pairwise additive interaction-site models. The parameters in the pairwise additive intermolecular models incorporate some of the nonpairwise additive effects of the surrounding medium and depend to some extent on the thermodynamic state of the system. AMBER [20], CHARMM [21], OPLS [22], and GROMACS [23] are examples of the most commonly used and better tested empirical force-fields. The

interaction sites in most of them have (united-atom model) systems considered force field (CHARMM [24–26], nucleic acids, the water molecule, the components, functions, which intramolecular interactions, bending, torsional, static interactions.

In these complex, increasingly large (in thousands), the evaluations, computationally expensive algorithms and the for MD simulations, long-range contributions in very large systems, slow and new algorithms currently being used in the simulations, such as $O(N)$ are just. The simulations can be accelerated by propagator algorithms studied systems [27–30], [31] with a three-step long-range interactions, steps in lipid bilayers, a cutoff (of about 10 Å).

To further reduce the hydrogen atoms to equilibrium values. The method employed here to solve the equations of motion, where the properties are

Since cells are in fixed conditions are fixed temperature and/or pressure, initial configuration needed in biological systems, thermostat [33]. The motions, sampling, and number of configurations, and number of

els to aid them to [1–3]. Pure lipid bilayers are the basic components of biomembranes.

membrane properties are of interest in the microscopic and experimental interest [4, 5].

Model biomembranes are systems governing their dynamics (MD) simulation of pure lipid bilayer systems, computer simulations of potential biomedical systems and references to components, such as lipids or proteins, or lack of detail available provides not only for the insights into crucial

component) membranes consider subjects as channels, surfactants, etc. To illustrate each most recent development, the polyunsaturated effect of surfactants on channels and their interactions in the

integration of the equations [4, 5]. This method is complex biological subject to the limitations of interaction potentials commonly used, the ion of interactions on polarizable pairwise additive interactive effects of the dynamic state of the CHARMM [23] and AMBER [24] force-fields. The

interaction sites in these models usually include all-atom descriptions, even though most of them have variants where groups of atoms are considered as single sites (united-atom models). In particular, the molecular and potential model used for the systems considered in this article was the recent version of the CHARMM all-atom force field (CHARMM27) for the different components of the biomembranes: lipids [24–26], nucleic acids [27], and proteins [28]. We used a rigid TIP3P model [29] for the water molecules, which is consistent with the force field chosen for the rest of the components. The intermolecular parts of the force fields are pairwise additive functions, which consist of simple Lennard-Jones plus Coulomb terms, while the intramolecular interactions consisted of bonded potentials (bond stretching, bond bending, torsional motions) and nonbonded potentials (Lennard-Jones and electrostatic interactions for atoms separated by more than two bonds).

In these complex biological systems, which usually are constituted by an increasingly large number of atoms (typically of the order of a few tens of thousands), the evaluation of the long-range electrostatic forces is the most computationally expensive part of the calculation. Recent developments of novel algorithms and the use of parallel machines, however, made these systems suitable for MD simulation studies. In systems with periodic boundary conditions, the long-range contributions are usually computed using the Ewald method. However, for very large systems, such as the one considered here, the Ewald summation is too slow and new algorithms with better scaling behavior have been developed and are currently being used. The particle mesh Ewald method [30], which has been used in the simulations reported in this article, and the fast multipole method (which scales as $O(N)$) are just a few examples [5]. Further improvement in the speed of the calculations can be achieved by using the so-called RESPA (reversible reference system propagator algorithm) algorithm, when multiple time scales are present in the studied systems [31]. For instance, the use of reversible multiple time step algorithm [31] with a three-stage force decomposition (into intramolecular, short-range, and long-range intermolecular interactions) permits the use of considerably larger time steps in lipid bilayer simulations. The short-range forces are usually computed using a cutoff (of about 10 Å) and methods like the minimum image convention [4, 5].

To further improve the efficiency of the calculations, the motions involving hydrogen atoms of the different molecules are usually constrained to their equilibrium values. The SHAKE/ROLL and RATTLE/ROLL methods [32] have been employed here to use a longer time step in the integration of the classical equations of motion, when those fast degrees of freedom are not expected to be relevant for the properties analyzed.

Since cells are usually constrained to an environment where the ambient conditions are fixed, MD simulations are usually performed at constant temperature and/or pressure with flexible simulation so the system is able to evolve from an initial configuration to its equilibrium state. The precise control of temperature needed in biological systems can be obtained by the use of the Nosé–Hoover chain thermostat [33]. In this case, the MD simulations solve the extended equations of motions, sampling the canonical (in a system with constant volume, temperature, and number of particles) or the isothermal-isobaric (constant pressure, temperature, and number of particles) ensembles [32].

The simulations of the complex biological systems reported in this discussion were performed using the recently developed PINY-MD computational package [34], which includes all the aforementioned new methodologies.

PURE LIPID BILAYERS: LIPIDS WITH HIGHLY UNSATURATED CHAINS

Fatty acids with multiple unsaturations or double bonds are quite abundant in brain gray matter, synaptic membranes, retinal tissue, and in the olfactory bulb [35–37]. The importance of polyunsaturated lipids, however, seems not to be limited to a mere structural role. In some situations polyunsaturated lipids are needed for the proper function of membrane embedded proteins, such as in the case of the G-protein coupled visual receptor rhodopsin [38]. By modifying the stability of Metarhodopsin II (MII) vs. Metarhodopsin I (MI), which are intermediate molecular forms of rhodopsin in the cascade that follows the absorption of a photon, the content of docosahexaenoic fatty acid (DHA) has been shown to affect rhodopsin's function [37–41]. Polyunsaturated fatty acids can also modify the activity of receptors by acting as ligands. For instance, the DHA has been recently identified as a ligand for the retinoid X receptor (RXR) in mouse brain, indicating that DHA may influence neural function through the activation of an RXR signaling pathway [42].

In simple model phospholipid bilayers, the presence of (*cis*) double bonds in one or both of the lipid fatty acid chains is known to affect a number of physical properties of the membranes. Examples of these effects are the low main order-disorder phase transition temperatures [43, 44], the enhanced permeability to water and small solutes [45, 46], the enhanced elasticity or decrease in area compressibility modulus [47–49] etc. The microscopic origin of these properties is, however, far from being well understood and although classical molecular dynamics simulation studies have been extensively used to investigate model membranes, earlier studies of water-lipid phosphatidylcholine systems in the lamellar phase were restricted to disaturated lipids [3] or lipids with a low degree of unsaturation [12, 24, 50]. Very recent MD simulation studies of a 1-stearoyl- 2-docosahexaenoyl- sn-glycero- 3-phosphocholine (SDPC, 18:0/22:6ω3 PC) lipid bilayer in the fluid lamellar phase [11, 51, 52] have improved our knowledge of the effect of highly polyunsaturated chains on the structure and dynamics of model membranes. This study was carried out at constant temperature ($T = 30^\circ\text{C}$) and pressure ($p = 1 \text{ atm}$) in a fully hydrated membrane consisting of 14,371 atoms (64 lipids and 1761 water molecules) [11].

In Fig. 1 (panel a), we show a snapshot of the SDPC lipid bilayer at the beginning of the equilibrium period, after a long (1.8 ns) equilibration period. The presence of the polyunsaturated chains (in green), which have the tendency to visit the lipid–water interface, increase the disorder of the membrane [11, 43, 51, 53, 54]. This trend was found also to enhance the interaction of water molecules with the end-carbon-atoms (and in general with the whole chain) of the polyunsaturated tail [11]. The different behavior of the polyunsaturated chains compared to that of the better studied saturated chains is due to a different intramolecular conformation and dynamics [11, 55, 56]. In particular, for the molecular bonds located between two (*cis*) double bonds, the dihedral angle distributions present two symmetric maxima

at $\pm 120^\circ$, which saturated chains do not, being the one with the lowest conformational entropy. The conformations of the polyunsaturated chains are mainly due to the presence of the *cis* double bonds, which are found in 66% of the lipid chains, since consecutive double bonds have a fraction of $1/2$ of the probability of being in the same conformation, where such a situation is not possible for inhomogeneous chains. The intramolecular dynamics of the polyunsaturated chains are mainly due to the different molecular conformations of the *cis* double bonds, which are given by the different conformations of the chain [51]. The different conformations of the *cis* double bonds are due to the different theoretical models used. In particular, we have used a saturated chain obtained by a disaturated chain with a double bond, and their covalently bonded atoms have angles close to 180° . The saturated chain region, the more ordered region, the less straight and more saturated chains. On the other hand, the chain were only partially saturated chain.

The tendency of the polyunsaturated chains to visit the lipid–water interface does not seem to be related to the difference between lipid bilayers with disaturated and polyunsaturated chains, but with the polar part of the lipid bilayer being more organized [11, 51, 52].

ed in this discussion
nputational package

SATURATED

re quite abundant in
e olfactory bulb [35–
not to be limited to
s are needed for the
the case of the G-
e stability of Metar-
ermediate molecular
on of a photon, the
o affect rhodopsin's
he activity of recep-
ently identified as a
ting that DHA may
naling pathway [42].
(is) double bonds in
number of physical
he low main order-
ermeability to water
area compressibility
ies is, however, far
ly dynamics simulation
anes, earlier studies
e were restricted to
on [12, 24, 50]. Very
noyl- sn-glycero- 3-
fluid lamellar phase
ly polyunsaturated
is study was carried
) in a fully hydrated
molecules) [11].

bilayer at the begin-
n period. The pres-
endency to visit the
[43, 51, 53, 54]. This
ecules with the end-
nsaturated tail [11].
to that of the better
conformation and
cated between two
symmetric maxima

at $\pm 120^\circ$, which correspond to the so-called *skew*[±] conformations. In contrast, in saturated chains they can adopt three conformations: *gauche*[±] and *trans*; the latter being the one most energetically favorable. Calculations of the different conformations of the DHA chain [11] indicated that the helical and angle-iron conformations of the region of the polyunsaturated chains comprising three consecutive *cis* double bonds are quite stable for the studied thermodynamic state, representing 66% of the lipids. These conformations allow a relatively tight packing of the chains since consecutive *cis* double bonds are parallelly oriented. Nevertheless, a significant fraction of molecules (34%) with conformations (hairpin and other hairpin-like) where such a tight packing is not possible was observed. This leads to a high degree of inhomogeneity in the system. In fact, the results obtained for the conformations and intramolecular dynamics indicated a broad distribution of projected area per (polyunsaturated) chain and fairly large local fluctuations for transitions between the different molecular conformations.

Calculation of the experimentally measurable (by NMR) orientational order parameter profiles from the MD simulations resulted in values for the polyunsaturated chains significantly lower than those for the saturated chain [11]; in good agreement with experiment [57]. To illustrate these differences, we show in Fig. 2(a) orientational order parameter profiles for the two acyl chains of the SDPC lipid, which are given by, $S_{CD}(n) = \frac{1}{2}(3 \cos^2 \beta_n - 1)$, where β_n is the angle between the orientation of the vector along a C–H bond of the n -th carbon atom of the saturated and/or the polyunsaturated chains and the bilayer normal. One of the advantages of computer simulation is that it allows one to calculate separately the different contributions to the order parameter profiles from the individual lipids with specific conformations, for instance, of the molecular segments comprising three consecutive *cis* double bonds of the polyunsaturated chains located at different positions along the chain [51]. By doing so, one can get insights into the molecular origin of the different theoretical and experimental findings on these complex organized systems. In particular, we plot in Fig. 2(b) the partial order parameter profiles for the saturated chain obtained as a function of the configuration of the region of the polyunsaturated chain close to the headgroup [51]. Figure 2 (b) shows that different polyunsaturated conformations have a distinct effect on the orientational order of their covalently bonded (saturated) chains. Individual conformations of the dihedral angles close to the lipid headgroup produce differences in the lower region of the saturated chain (Fig. 2(b)), in agreement with experimental observations [54]. In this region, the more linear structures (angle-iron and helical) increase the order, whereas the less straight conformations (hairpin and other) decrease the order of the saturated chains. Contrarily, the order parameters for the upper part of the saturated chain were only slightly changed as a function of the structure of the polyunsaturated chain.

The tendency of the polyunsaturated chains to visit the lipid–water interface does not seem to strongly modify the interactions amongst lipid headgroups or between lipid headgroups and water molecules at the membrane surface compared with disaturated lipid bilayers [11, 52]. At the interface, which constitutes the most polar part of the membrane, lipid headgroups and water molecules are strongly organized [11, 52]. This organization is not only found along the bilayer normal,

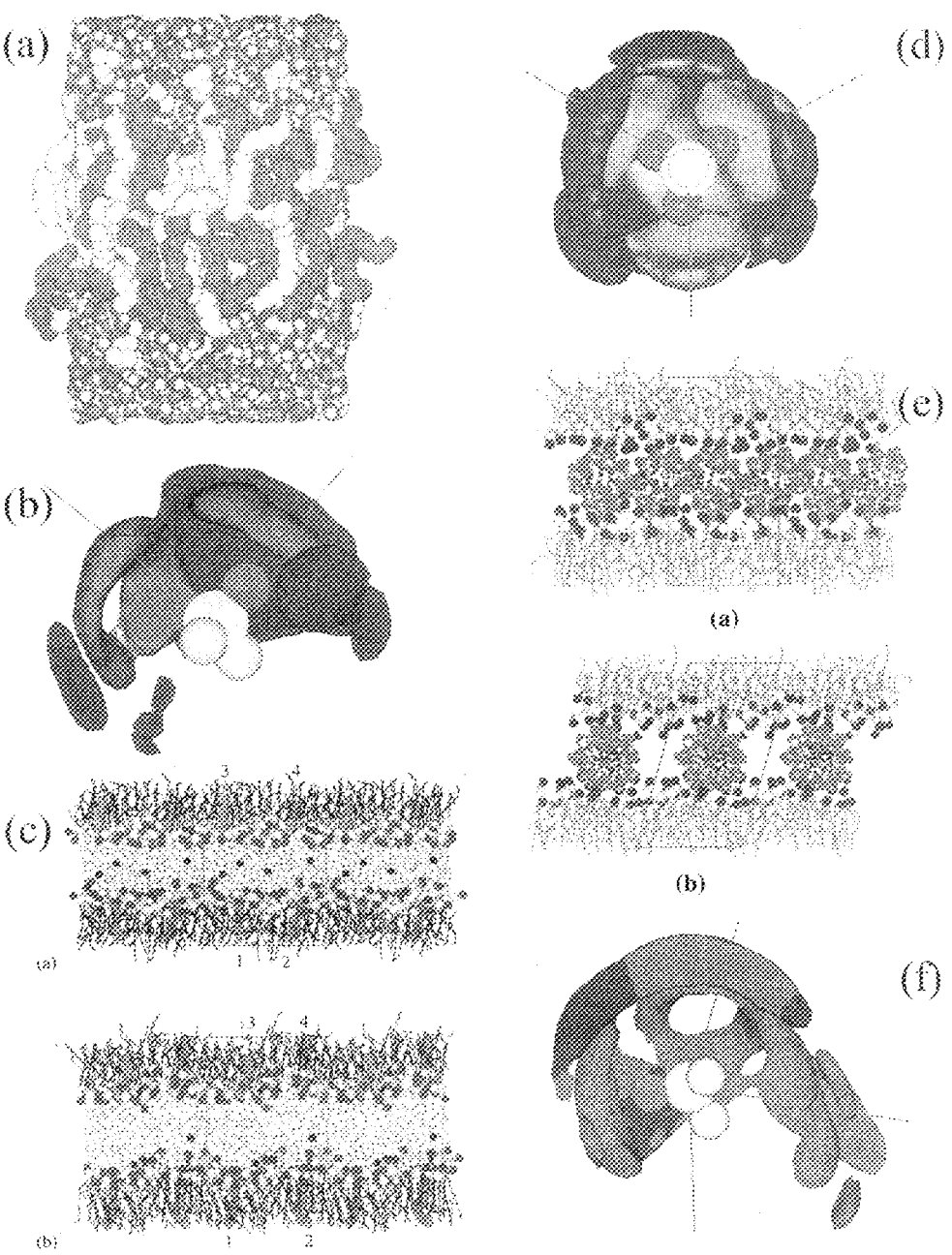


Fig. 1. (panels a-f). Panel a: Configuration of the highly unsaturated model SDPC lipid bilayer system after 2 ns at constant pressure and temperature (isothermal-isobaric ensemble). Only the molecules in the simulation cell are shown. Molecules are depicted by their atomic van der Waals radii, and, for the sake of clarity, the hydrogen atoms of the lipids are not displayed. The color code for the lipids is as follows:

where the water group $P^{\prime} \rightarrow N^{\prime}$. At the interface to minimize the this network, via bridges among the molecular distribution (in red) and nitrogen (red) water phosphate group. Some same molecule free and nonfree, for instance, in PCs, which lead and counterion systems [58], or in DNA/charge

The effect issue in memb

nitrogen (blue), phosphate group carbon atoms of the water molecules is

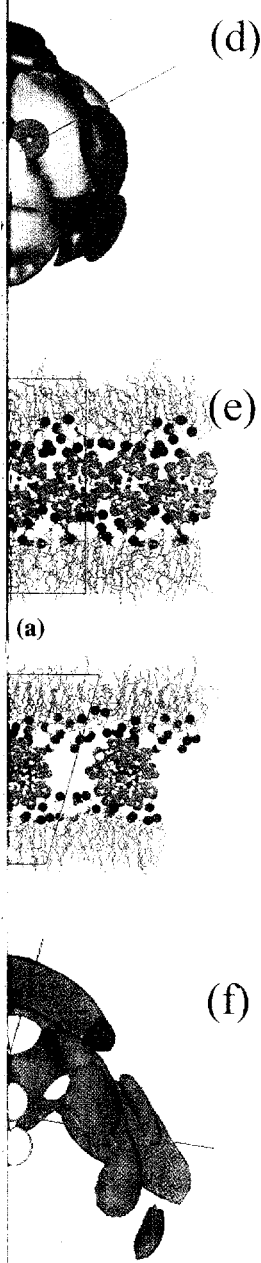
Panel b: Three water molecules (red) phosphate group is as follows: phosph

Panel c: Snapshot and after 3.2 ns of drawn as spheres. scheme is N, blue; and Na ions are numbered for visual clarity.

Panel d: Average oxygen atoms (green) sulfate group is anionic and the es

Panel e: Cont different views and head group P and atom coloring sch The water molecu of the central sim

Panel f: Three oxygen atoms are lipid (DMTAP) and the water density the nonbonded at



where the water molecules are polarized to counteract the effect of the SDPC headgroup $P^- \rightarrow N^+$ dipoles, preferentially oriented forming 70° with the bilayer normal. At the interfacial plane, the lipid headgroups form a network of interacting moieties to minimize the electrostatic interactions via $P^- \dots N^+$ charge pairs [11, 13, 52]. In this network, water molecules interact with the lipid headgroups and even form bridges among them. This behavior is illustrated in the three-dimensional intermolecular distribution (see Fig. 1, panel b) of the oxygen atoms of the water molecules (in red) and nitrogen atoms of the lipids (in blue) around the phosphate groups by the (red) water rings around the non-bonded oxygen atoms (in gray) of the phosphate group. Similar distances are preferentially adopted by those atoms within the same molecule [11], which agrees with the similarities found in the properties for free and nonfree ions in lipid bilayers. Examples of this phenomenon can be found, for instance, in the screening of charges in DNA complexes or planar surfaces of PCs, which leads to forces that does not depend critically on whether the phosphate and counterion are bonded, as in PCs, or not, as in DNA/tetramethylammonium systems [58], or in the equal screening of DNA charges by neutral and charged lipids in DNA/charged-lipid-bilayer complexes [59].

SURFACTANT IN A BIOMEMBRANE

The effect of foreign molecules on phospholipid membranes is a long standing issue in membrane science. Surfactants form an important class of such foreign

nitrogen (blue), phosphorus (yellow), oxygen (red), hydrogen (white), and carbon (gray) atoms. The carbon atoms of the polyunsaturated chains of the lipids are highlighted in green. The color code for the water molecules is as follows: oxygen (blue) and hydrogen (white) atoms.

Panel b: Three-dimensional average intermolecular density isosurfaces of the oxygen atoms of the water molecules (red surface) and the nitrogen atoms of the lipid molecules (blue surface) around the phosphate group of the SDPC molecule. The color code for the phosphate group of the lipid molecules is as follows: phosphorus (yellow), non-bonded oxygen (red), and bonded oxygen (gray) atoms.

Panel c: Snapshots of the configuration of the DMPC/SDS mixed system near the beginning (a), and after 3.2 ns of the simulation. The surfactant molecules and the lipid headgroup P and N atoms are drawn as spheres, while the lipid chain atoms and water molecules are drawn as sticks. The atom coloring scheme is N, blue; P, yellow; S, gray; O, red; C (surfactant), green; C (lipid), black; water molecules, blue; and Na ions, deep blue. The lipid and surfactant H atoms are not drawn. The surfactant DS chains are numbered for reference and the system is replicated once on both sides of the central simulation cell for visual clarity.

Panel d: Average density isosurfaces of the lipid headgroup nitrogen atoms (blue), and the water oxygen atoms (green) around a representative sulfate headgroup of the surfactant chain. The surfactant sulfate group is at the center of the figure, where the central sulfur atom is drawn in yellow, while the anionic and the ester oxygen atoms are drawn as red and gray spheres, respectively.

Panel e: Configuration of the DMPC/DMTAP-DNA complex after 5.5 ns of MD simulation. Two different views are shown: (a) perpendicular to, and (b) along the DNA axis. The DNA and the lipid head group P and N atoms are drawn as spheres, while the lipid chain atoms are drawn as sticks. The atom coloring scheme is N, blue; O, red; P, yellow; C (DNA), gray; C (lipid), green and H, dark gray. The water molecules and the lipid H atoms are not shown and the system is replicated once on both sides of the central simulation cell for visual clarity.

Panel f: Three-dimensional density isosurfaces of the lipid head group nitrogen atoms and the water oxygen atoms around a representative DNA phosphate group. The probability densities of the cationic lipid (DMTAP) and neutral lipid (DMPC) nitrogen atoms are drawn in red and blue, respectively, while the water density surface is drawn in green. The DNA phosphate group is at the center of the figure with the nonbonded and bonded oxygen atoms drawn as red and gray spheres, respectively.

PC lipid bilayer system
only the molecules in the
radii, and, for the sake
the lipids is as follows:

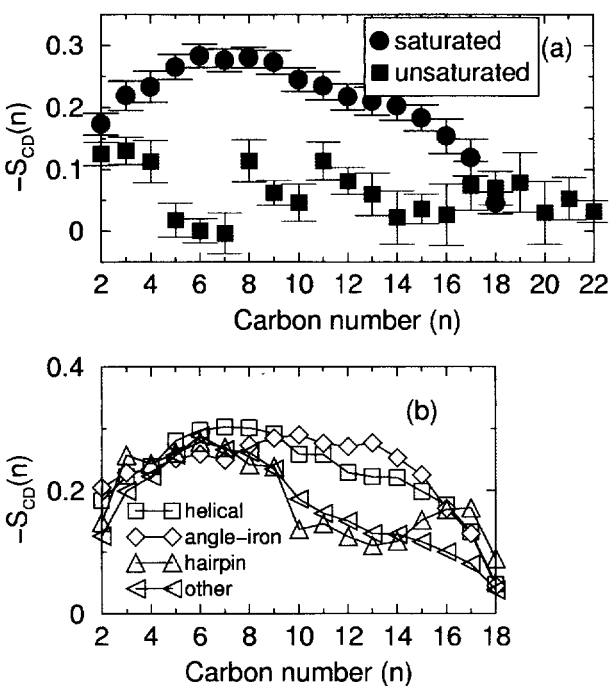


Fig. 2. (a) Orientational order parameter ($S_{CP}(n)$) as a function of the position of the carbon atom along the chains. The result of the saturated (black circles) and polyunsaturated (squares) chains are plotted separately. Error bars represent the standard deviations. (b) Orientational order parameter profiles of the SDPC saturated chains obtained by averaging over different conformations of the region of the polyunsaturated chains close to the headgroups. The lines are visual guides.

molecules. The study of phospholipid/surfactant mixed bilayer systems is important not only for many useful biochemical processes, such as, membrane solubilization [60–62], and protein extraction [63], but also as model systems for understanding crucial issues, such as, the structure and dynamic properties of such complex systems [64–66], and the partition of these foreign molecules in the bilayer matrix [67]. Besides, surfactants, being the major constituents of detergents, are released everyday into the environment, particularly into natural water. Therefore, the questions of how surfactants interact with biomembranes, and influence their properties are central issues for both toxicology and environmental science.

Due to technical limitations, it is difficult to carry out well-controlled experiments on lipid bilayer systems with additives. Klose and coworkers [60, 64–66, 68] have studied in detail the properties of mixed multilayers containing palmitoyloleoyl-phosphatidylcholine (POPC) lipids and non-ionic surfactants $C_{12}E_n$ (monodecyl ethers of poly(oxyethylene) glycols), using X-ray, neutron diffraction and NMR.

Because of the complex nature of the problem, very little theoretical modeling has been attempted in this area [67, 69]. Atomic based computer simulations can

play a powerful level, and are the due to the inherent membranes contained were a few attempts.

We report the formation of a lamellar phase containing a mixture of membrane/surfactant and SDS surfactant molecules. The

In Fig. 1 (p) near the beginning showed how the due to the presentations between the headgroups were. The overall distance is similar to that chains were found groups of the lipid interact with the of the PC headgroups were calculated between the negative $\text{N}(\text{CH}_3)_3^+$ ends of the bound to the surface. The strong interaction $\text{P}^- \rightarrow \text{N}^+$ dipole-dipole bilayer (as shown by the vector and the large

Ion channels in membranes [72], the transmission of signaling in nerve. Even though the model is based on a single set of parameters, it is able to predict the behavior of a wide variety of ion channels.

ated with function. Since only atomic resolution is available, a minimalist protein that can be studied in more detail will be of great interest.

play a powerful role in elucidating the properties of these systems at a microscopic level, and are therefore considered as natural complements to experiments. However, due to the inherent complexity, there are practically no atomistic simulations of lipid membranes containing long chain additives, such as surfactants. Only recently there were a few attempts at MD studies on phospholipid-surfactant mixtures [70, 71].

We reported long all-atom MD simulations of the lamellar phase of a membrane/surfactant mixture containing dimyristoylphosphatidylcholine (DMPC) lipids and SDS surfactants [70]. The simulation was carried out at 30°C, with a mol fraction of 6.6% surfactant. The system contained 60 lipids, 4 SDS, and 1641 water molecules. The calculated properties of the mixed system were compared with the lamellar phase of pure DMPC lipids, and with available experimental data.

In Fig. 1 (panel c), we show snapshots of the configuration of the mixed system near the beginning and after 3.2 nanoseconds of the simulation. These snapshots showed how the nearly flat interface at the beginning had undergone perturbations due to the presence of the surfactants. Such perturbations indicated strong interactions between the surfactant and lipid headgroups. The location of the surfactant headgroups were obtained from the electron density profiles, as shown in Fig. 3. The overall distribution of the profiles for the lipid in the mixed system (Fig. 3(b)) is similar to that of the pure system (Fig. 3(a)). The headgroups of the surfactant chains were found to be located slightly deeper into the bilayer, near the carbonyl groups of the lipids. To obtain how the negatively charged surfactant headgroups interact with the zwitterionic phosphocholine (PC) groups, local density isosurfaces of the PC headgroup nitrogens and water molecules around the sulfate headgroups, were calculated (Fig. 1, panel d). These distributions reveal strong interactions between the negatively charged surfactant headgroups and the positively charged $\text{N}(\text{CH}_3)_3^+$ ends of PC groups. It was also shown that the lipid $\text{N}(\text{CH}_3)_3^+$ groups were bound to the surfactant headgroups either directly or bridged by water molecules. The strong interactions between the surfactant and lipid headgroups lead the $\text{P}^- \rightarrow \text{N}^+$ dipole vector of the lipid headgroups to reorient toward the interior of the bilayer (as shown in Fig. 4), with $\theta > 90^\circ$, where θ is the angle between $\text{P}^- \rightarrow \text{N}^+$ vector and the bilayer normal.

MEMBRANE PROTEINS: ION CHANNELS

Ion channels are membrane proteins that regulate the flux of ions across cell membranes [72]. They are present in membranes of all cells and are responsible for the transmission of signals in many processes such as, excitation and electrical signaling in nerve and muscle synapses, detection of sounds and visual images, etc. Even though they play a fundamental role in biology, the structural motifs associated with function are just starting to emerge [72–79].

Since only a few of the structures of these ion channels have been solved with atomic resolution [73, 74, 80], experimentalists have approached this issue by studying minimalistic (simplified) synthetic peptide [81] channels or the sections of the protein that constitute the pore region of large native channels [77, 82–84] to get more insights into their function. These smaller systems, which still retain some or

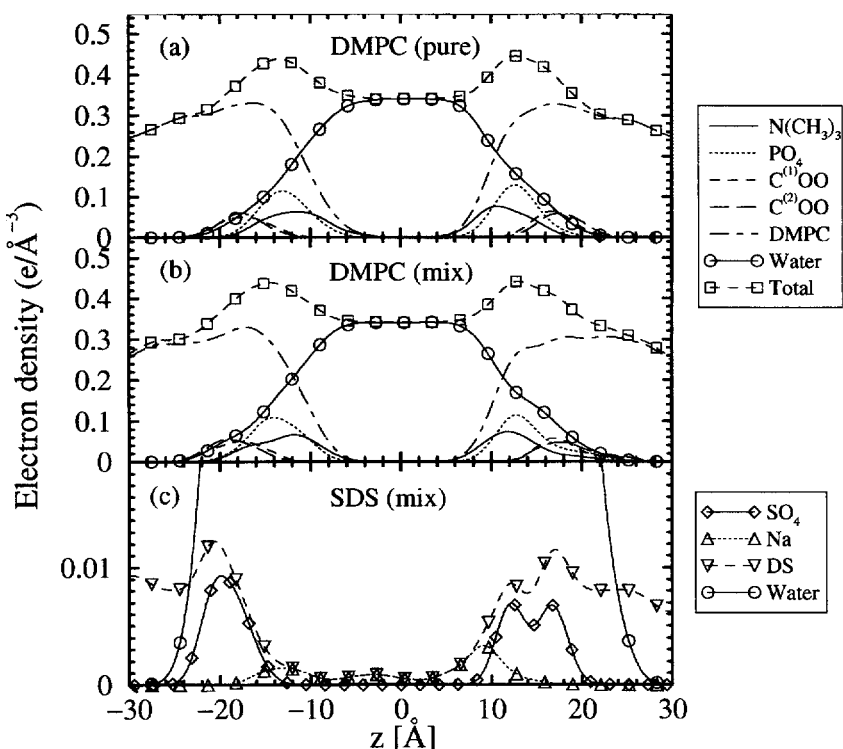


Fig. 3. Electron density profiles measured along the bilayer normal, z , for different components of the DMPC lipid in the pure (a), and in the mixed system (b). The total electron density distributions and that arising from water are also shown. The density profiles of the surfactant headgroups (SO_4^-), dodecylsulfate chains (DS), and the sodium counterions in the mixed system are shown in (c). The distribution for water is added in (c) for clarity.

most of the functionality of the channels, have been the focus of attention of atomistic molecular dynamics simulations [85–89].

The incorporation of relatively large membrane proteins, such as ion channels, in membranes is expected to modify the physical properties of the lipid bilayer. However, due to the fundamental importance of these proteins most of the effort of the experimental and theoretical works has been devoted to the study of the effects of the lipid environment on the structure, dynamics, and function of membrane proteins. Two cases are of particular interest: the effects on the activity of the gramicidin A channel, which due to its simplicity has been extensively studied theoretically and by computer simulations [90–92], and the effect of specific phospholipids, in particular those with unsaturations [11], on the activity of the G-protein coupled visual receptor rhodopsin [39–41]. The key factor in this behavior seems to be the hydrophobic mismatch, i.e., the difference between the hydrophobic length measured perpendicular to the membrane surface of the lipid bilayer and the protein. The membrane curvature seems also to be an important factor, and lipids promoting inverted hexagonal phases have been shown to be fundamental in some systems.

Recent experiments on membrane peptides have shown that the structure of membrane proteins in the membrane protein system [93, 94] and the transmembrane domain can increase the orientation of the peptide performed on a peptide with 10 amino acid residues at each position of the membrane region (membrane bilayer). The lipid bilayers no longer rotate around the interface by rotation around the plane due to the presence of the peptide, even though a membrane peptide, the forces of which are not known, the time scale of the spectroscopy studies, however, indicate that the bilayer in a system of membrane proteins can differ. Differences obtained in the topology of the peptide

To investigate physical properties of membrane homopolymer [83, 84] were recorded.

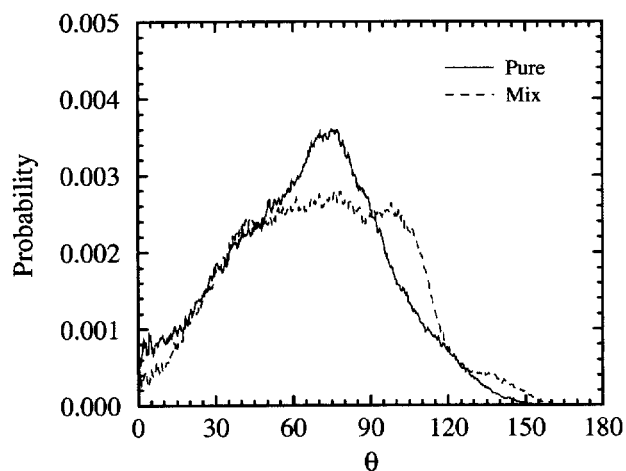


Fig. 4. The orientation distribution of the lipid $P^- \rightarrow N^+$ headgroup dipoles with respect to the bilayer normal, z , for pure DMPC lipids in L_α phase (solid line) and that in the mixture (dashed line).

Recent experiments have been directed to the study of the influence of simple membrane peptides on the membrane properties in an effort to get more insights into the structure and dynamics of model membranes. The effect of incorporating membrane proteins into lipid bilayers changes the phase behavior of the water-lipid system [93, 94] and can even promote nonbilayer phases [93], for instance, single transmembrane peptides decrease the temperature of the phase transition and increase the orientational order of the lipid chains [95]. Other NMR experiments performed on a mostly hydrophobic cationic peptide with two hydrophilic Lys^+ residues at each peptide end showed that the order parameters of the hydrophobic region (membrane interior) were not significantly modified by the peptide in DMPC lipid bilayers nor in DMPC/DMPS (5:1) but that the peptide affects the membrane interface by rotating the headgroup dipoles in a direction away from the membrane plane due to the (sign of the) "bound" surface charges [96]. In these experiments, even though a major influence is expected to occur in the lipids located closer to the peptide, the formation of lipid-protein complexes are usually ruled out at least in the time scale of the NMR experiments ($\approx 10^{-5}$ s) [96]. Systematic NMR and ESR spectroscopy studies using hydrophobic polypeptides of different lengths [93], however, indicate that peptides can induce a hydrophobic mismatch that perturbs the bilayer in a systematic manner (in an effort of the lipids to reduce this mismatch). Differences obtained for peptides with different shapes indicate also that the topology of the peptide surface modulates the effect of hydrophobic mismatch [93, 95].

To investigate the effect of the presence of ion-channel forming peptides on the physical properties of the lipid environment, atomistic MD simulations of the transmembrane homopentameric bundle of the α -helical M2 segments which are believed to form the pore region of the nicotinic acetylcholine receptor (nAChR) ion channel [83, 84] were recently performed [89]. The nAChR is the neurotransmitter-gated ion

different components. The total electron density profiles of the cationic counterions are shown in (c) for clarity.

attention of atom-

such as ion channels, of the lipid bilayer. Most of the effort of study of the effects of membrane activity of the gram-negative bacteria has been theoretically studied for phospholipids, in G-protein coupled receptor seems to be the bic length measured and the protein. The lipids promoting in some systems.

channel responsible for the rapid propagation of electrical signals between cells at the nerve-muscle synapse [72]. Previous simulation studies on the nAChR were focused exclusively in protein-protein interactions of simplified models or the effects of α -helices environment on the secondary structure. The peptide bundle was embedded in a fully hydrated DMPC lipid bilayer in the fluid lamellar phase, L_α , at ambient conditions ($T = 303$ K and $p = 1$ atm) with a lipid/peptide molar ratio of 19:1 [89]. The M2 segments are characterized by the sequence GSEKMSTAISVLLAQAVFLLLTSQR and correspond to the δ subunit of the native nAChR ion channel of *Rattus norvegicus* [84].

In Fig. 5, we show a snapshot of the simulated system after 2 ns. Preliminary results [97] indicate that the main effect of the incorporation of the ion channel into the DMPC lipid bilayer consists of an increase of the bilayer thickness and of the orientational order of the DMPC lipid acyl chains. Other effects include: perturbation of the orientation of the lipid headgroup $P^- \rightarrow N^+$ dipoles at the membrane

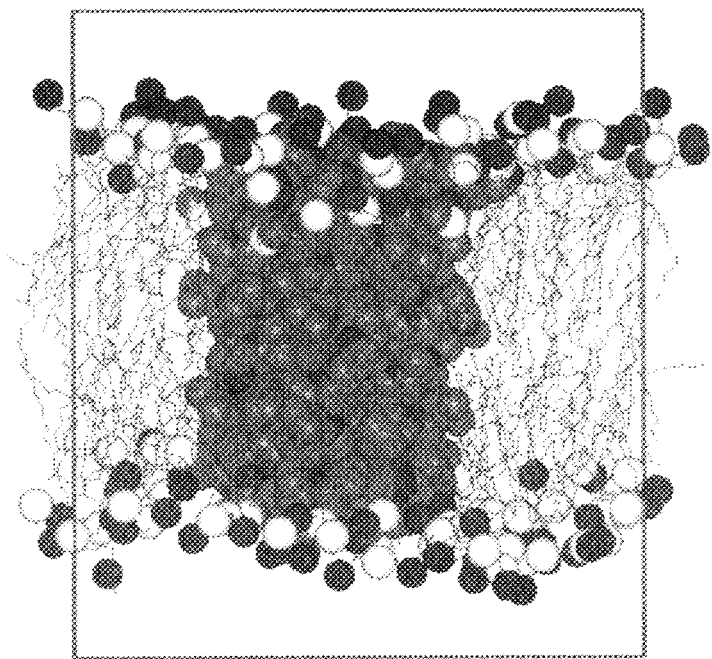


Fig. 5. Configuration of the pentameric bundle of the M2 segments, forming the pore of nicotinic acetylcholine receptor ion channel, in a DMPC lipid bilayer after 2 ns. The lipid molecules are shown as balls and sticks for clarity except the nitrogen and phosphorus atoms of the headgroups displayed as black and light gray spheres, respectively. The water molecules and hydrogen atoms are not shown for clarity. The M2 helices are shown in dark gray, except the sulfur (light gray) and nitrogen (black) atoms. The radii of the spheres correspond to the atomic van der Waals radii of the different species. The C-terminus [synaptic or extracellular, see Ref. 84] is located at the bottom of the bundle.

Due to the of interactions t viral carriers re out that help ra [115]. Atomistic structural and o of the problem, to study such sy lipid-DNA con was carried out simulation was c 1003 water mol system setup an

Figure 1 (p)
seconds of simu
I is the structur
developed near
nearly flat inter

ls between cells at the AChR were focused on the effects of α -helices embedded in a L_{α} , at ambient conditions of 19:1 [89]. The M2 helix of *Rattus norvegicus*

after 2 ns. Preliminary studies of the ion channel into the membrane thickness and of the effects include: perturbations at the membrane

interface; and a change in the analyzed properties as a function of the distance of the lipid from the bundle center of mass. The behavior of the lipids located at the two different leaflets differed. Some of these effects seem to be associated with the formation of lipid–protein complexes. Lipid–peptide interactions, mainly via Lys⁺, which is located at the external surface of the peptides, with the lipid phosphate groups, have also been observed.

LIPID–DNA COMPLEXES

Human gene transfer is an important clinical strategy in which a segment of extracellular DNA is transferred to the nucleus of cells to replace or add genes [98–100]. Gene transfer involves the delivery of a cassette made up of one or more genes and the sequences controlling their expression to target cells. At present, the most common method of gene delivery uses viral-based carriers of DNA [98, 101, 102]. It has been known for some time that binary mixtures of suitable cationic and neutral lipids can form stable complexes with DNA and hence can potentially be used as synthetic carriers of DNA [103]. Recently, the study of lipid–DNA complexes has received considerable attention [99–102, 104–116]. X-ray studies by Safinya *et al.* [104, 105] discovered that mixtures containing the unsaturated neutral DOPC (dioleoylphosphatidylcholine) and the cationic DOTAP (dioleoyltrimethylammonium propane) lipids form a novel multilayer structure with alternating lipid bilayers and DNA monolayers, in which the DNA chains form a two-dimensional smectic phase, intercalated between lipid bilayers. Rädler and coworkers [106, 107] used binary mixtures of the saturated neutral and cationic lipid DMPC and DMTAP to complex with DNA. These intercalated complexes exist in two lamellar phases, the gel phase (L_{β}^g) at low temperatures and the fluid-like lamellar phase (L_{α}^f) at higher temperatures.

Due to the lack of understanding of the lipid–DNA complexes, and the nature of interactions between the DNA and the lipids, the development of synthetic non-viral carriers remains preliminary. Few theoretical calculations have been carried out that help rationalize the observed structures of the lipid–DNA complexes [111–115]. Atomistic based MD simulations can play an important role in elucidating the structural and other properties of such systems. However, due to the complex nature of the problem, no atomistic computer simulation study has been attempted so far to study such systems. Only recently, we performed an all-atom MD simulations of lipid–DNA complexes containing DMPC and DMTAP lipids [59]. This simulation was carried out in the liquid crystalline L_{α}^f phase of the complex ($T = 50^{\circ}\text{C}$). The simulation was carried out at an isoelectric point containing 24 DMPC, 20 DMTAP, 1003 water molecules, and a DNA duplex d(CCAACGTTG)₂. The details of the system setup and simulation details can be found elsewhere [59].

Figure 1 (panel e) shows the configuration of the system after a long 5.5 nanoseconds of simulation. The most interesting and important feature to note from Fig. 1 is the structure of the lipid–DNA interface. It is clear that significant undulations developed near the lipid head group region of the interface as compared to the nearly flat interface of the lipid bilayer.

nts, forming
DMPC lipid
complexes for clar-
ification. The
displayed
molecules and
atoms. The
radii of the
Ref. 84] is

Calculation of the three-dimensional local density isosurfaces of the lipid head group nitrogen atoms as well as the water molecules around the DNA phosphate groups (Fig. 1, panel f) reveal that a large fraction of the cationic lipids, are bound to the DNA phosphate groups either directly or bridged by water molecules. However, the most interesting feature was the significant population of the zwitterionic PC head group nitrogens of DMPC in proximity to a DNA phosphate group. Our results predicted the existence of TAP and PC groups with about equal probability around the DNA phosphates. From a similar estimation, we found that there are roughly 2.5 water molecules per non-bonded DNA phosphate oxygen atom within a typical nearest neighbor distance of $\sim 3.3 \text{ \AA}$, which confirms the existence of water molecules bridged between the lipid head groups and the DNA phosphates.

The reason behind such an apparently surprising distribution as shown in Fig. 1 (panel f) is the attractive electrostatic interaction between the cationic TAP head group and the anionic phosphate of the zwitterionic PC head group of DMPC. In Fig. 6 we show a snapshot from the simulation illustrating the lipid–lipid and lipid–DNA contacts (salt bridges). For clarity, we have shown only the N^+ and P^- atoms of the PC and N^+ atoms of the TAP groups corresponding to one monolayer and the phosphate groups of the DNA, which are close to that layer. Figure 6 clearly shows the existence of three distinct types of contact bridges as marked by circular regions. *Region 1*, shows a P^- – N^+ – P^- N^+ type of bridge between the PC groups, typical of a pure lipid bilayer structure [13]. Similar bridged configurations are identified in *Region 2*, where the N^+ of the PC group is replaced by the cationic N^+ of the TAP group. The existence of such configurations unambiguously demonstrates the presence of strong electrostatic interactions between the PC and TAP head groups. This leads to the formation of contact pairs of DMPC-DMTAP lipids with the P^- end of the P^- – N^+ dipole approximately at the same distance ($\sim 4.5 \text{ \AA}$) from the PC head group N^+ as from the N^+ of the TAP group. Such interactions also induce a change in orientation of the P^- – N^+ head group dipoles of DMPC with the N^+ part pointing away from the bilayer plane and hence coming into more effective contact with the anionic DNA phosphate, as illustrated in *Region 3* of the snapshot. The explicit arrangements of the atoms in these three regions are shown in the insets of Fig. 6.

This study showed that the current generation of simulation methodologies and force fields have the ability to offer valuable insights into such complex systems with potential biomedical applications.

PERSPECTIVES

The examples considered in the previous sections illustrate the current ability of computer simulations to describe model membranes of a considerable degree of complexity. The membranes of cells are, however, composed of a heterogeneous mixture of various components and one would like also to learn about their lateral organization. Recently, there have been a few attempts to study model systems with a mixture of lipids [117, 59] and special attention has been devoted to cholesterol [118–124] and its role in the formation of microdomains [125]. This is particularly

relevant since *cell* *membranes* *are* *heterogeneous*. *One* *example* *is* *cholesterol*, *which* *is* *an* *essential* *component* *of* *cell* *membranes*, *which* *is* *involved* *in* *the* *formation* *of* *microdomains* *in* *cell* *membranes*. *Cholesterol* *is* *able* *to* *interact* *with* *lipids* *and* *proteins* *in* *the* *membrane* *bilayer*, *thereby* *modulating* *the* *lipid* *arrangement* *and* *the* *membrane* *properties*. *Cholesterol* *is* *also* *involved* *in* *the* *regulation* *of* *membrane* *fluidity* *and* *function*.

aces of the lipid head the DNA phosphate onic lipids, are bound water molecules. How on of the zwitterionic phosphate group. Our out equal probability found that there are oxygen atom within the existence of water & phosphates.

ion as shown in Fig. 6, the cationic TAP head group of DMPC. In lipid-lipid and lipid-DNA the N^+ and P^+ atoms are one monolayer and layer. Figure 6 clearly is marked by circular the PC groups, typifications are identified the cationic N^+ of the TAP group. Figure 6 clearly demonstrates the d TAP head groups. AP lipids with the P^+ ($\sim 4.5 \text{ \AA}$) from the PC interactions also induce a PC with the N^+ part more effective contract of the snapshot. The shown in the insets of

in methodologies and complex systems with

the current ability considerable degree of an heterogeneous in about their lateral model systems with voted to cholesterol. This is particularly relevant since cholesterol seems to be crucial in the sorting of membrane heterogeneities. One example is the formation of the so-called lipid rafts [126] in plasma membranes, which act as platforms of adhesion and signaling. Even though this kind of model is still too complex for the present capabilities of atomistic scale computer simulations, the properties of mixed lipid bilayers can help understand the lateral organization of these membrane heterogeneities. An instance of the current efforts towards the study of such multicomponent systems with atomistic detail is

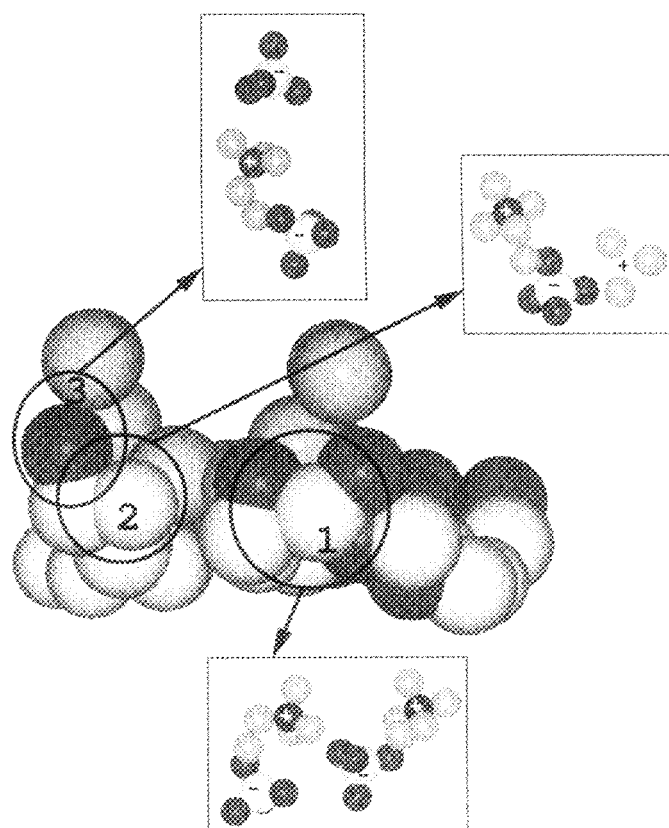


Fig. 6. A snapshot from the simulation illustrating how $N(CH_3)_3^+$ (black) and PO_4^3- (light gray) of the zwitterionic PC head groups and $N(CH_3)_3^+$ of the TAP groups interact with the phosphate groups (dark gray) of the DNA. *Region 1* shows $P^+-N^+-P^+-N^+$ contacts between the PC groups. *Region 2* shows substitution of N^+ of a PC group by the N^+ of a TAP group, while *Region 3* demonstrates how such substitution leads to change in orientation of the PC group, bringing it into close proximity with the DNA phosphate. For clarity, the spheres are drawn with artificially enhanced radii of 3.6 \AA (N) and 3.9 \AA (P). The insets show the explicit arrangement of the atoms in the PC and TAP groups as well as the DNA phosphate group within the three regions. Hydrogen atoms and water molecules are omitted for visual clarity.

the modeling of human bile, which consists of a mixture of phospholipids, bile salts, and cholesterol, and forms micelles under supersaturated conditions [127].

Lipid-protein and protein-protein interactions in membrane environments play a fundamental role not only in the folding of natural proteins or association of synthetic peptides but also in the mechanisms of action of toxins and antimicrobial peptides or other peptides with lytic activity, which are lethal to the cells. Peptide aggregation in membranes and the formation of pores is, thus, becoming a very challenging problem, for both computer and experimental studies. Recent experiments using novel X-ray methods to study peptide aggregation (at low concentrations) and its role in pore formation provide structural evidence that self-association of amphipathic helices at the membrane surface may be the crucial initial step toward bilayer destabilization and, consequently, the formation of pores [128]. The two state model proposed recently for the action of antimicrobial peptides [129], in contrast, reviews the latest experimental literature in the field and found no indication of helix association of peptides at the membrane interface for the intermediate state between a regime (at low lipid/peptide concentration) where the peptide adsorption at the interface occurs and a regime (at high lipid/peptide concentration) where the pores are formed. Similarly, in membrane protein folding, a reasonable scenario is the two stage model [130]. In a first stage, the helical regions of the protein or model (synthetic) peptides insert in the bilayer, and then oligomerization takes place. However, it is worth emphasizing that this thermodynamic model is just one possibility (reviewed in Ref. [131]) and that the process of insertion and assembly are far from being well understood.

Recent computer simulations demonstrate that processes such as spontaneous aggregation of phospholipids into bilayers or collective phenomena, such as the appearance of spontaneous undulations, can be followed and studied with atomistic detail. In particular, Marrink *et al.* [132] followed the formation of a DPPC lipid bilayer from a random configuration of lipids during 10–100 ns and identified the reduction and subsequent disappearance of transmembrane water pores as the rate-limiting process of the aggregation. The extension of the size of the system to lengths larger than the thickness of the bilayer permits the development of spontaneous undulations and, thus, the study of collective phenomena. Bending modes have been extensively studied and a spectral decomposition of the mesoscopic undulations and thickness fluctuation modes (into peristaltic, undulatory, and protrusions) was performed [133] and mesoscopic properties, such as the bilayer bending modulus, have been accurately calculated. Simulations show that the membrane properties in the long wavelength limit can be reproduced by continuum models. These two examples are illustrative of the latest achievement on time and length scales available for molecular dynamics simulations. These mesoscopic regimes reached nowadays by atomistic simulations were only available to simplified models. Among these models, those of the coarse-grain type [134, 135], for instance, which are adjusted to mimic a specific system instead of a general phenomenon, are still useful since they are significantly more efficient than atomistic models to study collective phenomena.

There are many issues from a more theoretical/methodological point of view that should be addressed, even though it is clear that most of the effort is being devoted to the modeling of more complex (multicomponent) systems. The main

concern is the experimental conditions and the system size on the important topic of pores up to mesoscopic scales. In the case of the surface tension, thus, depends strongly on the surface area per molecule, has been observed to depend on the deviations are proportional to the surface area per molecule in lamellar phases. This topic is being updated, 1

The past decade has seen a rapid development in the field of molecular dynamics along with the development of new methodologies. These methods have been applied to a wide range of problems in the frontier areas of biology and materials science. A significant amount of work has been made on the simulation of lipid membranes, an important membrane component. In the recent past, large-scale simulations have been performed on various systems, including forming ion-channels, DNA unwinding, and DNA gene transcription. These studies have shown excellent agreement with experimental results, and can provide valuable insights into the properties of such systems. In the past decade, molecular dynamics simulations have been used to probe even more complex systems, such as

This work was supported by the National Institutes of Health and the National Center for Research Resources (NPACI) San Diego Supercomputer Center.

1. *Structure and Function of Lipid Bilayers* (Lipowsky, R., Ed.), Marcel Dekker, New York, 1995.
2. Small, D. M. *Advances in the Molecular Dynamics of Lipid Research*, Marcel Dekker, New York, 1996.

ospholipids, bile salts, lipids [127].

These environments play roles or association of lipids and antimicrobial agents to the cells. Peptide toxins, becoming a very interesting subject. Recent experiments (at low concentrations) show evidence that self-assembly may be the crucial initial formation of pores [128].

Microbial peptides [129], and found no evidence for the intermediate state (where the peptide concentration) folding, a reasonable model for helical regions of the then oligomerization. A dynamic model is just a question of insertion and assembly

such as spontaneous phenomena, such as the studied with atomistic simulation of a DPPC lipid bilayer and identified the formation of pores as the rate-limiting step in the system to lengths of spontaneous bending modes have been found (bipolar undulations and protrusions) was bending modulus, have unique properties in the. These two examples are available for research nowadays by among these models, are adjusted to mimic useful since they are collective phenomena. From a physical point of view if the effort is being systems. The main

concern is the ability of computer simulations to reproduce experiments and experimental conditions. Due to the finite size of the computer simulations, the study of system size on the physical properties of the model membranes has always been an important topic [6, 17, 133, 136, 137]. The extension of temporal and spatial scales up to mesoscopic regimes has permitted the further evaluation of finite-size effects. In the case of the surface tension, for instance, earlier simulations [6] indicated that the surface tension decreases with increasing size of the systems. Surface tension, thus, depends strongly on surface area and a decrease in the surface compressibility has been observed due to undulatory modes [133, 136]. This effect, however, appears to depend on the stress conditions [136]. Even in very simple model systems large deviations are present between literature values for structural quantities, such as the surface area per lipid, due to the presence of fluctuations, inherent in disordered lamellar phases. Recently, these structural parameters and material properties are being updated, reviewed, and adjusted, and are becoming available [48, 138].

CONCLUSION

The past decade has yielded revolutionary advances in computer hardware technology along with concomitant development of state-of-the-art simulation methodologies. These two factors have enabled the successful application of computer simulation methods in general, and molecular dynamics (MD) in particular, in frontier areas of biomedical research. In this article, we reviewed recent progress that has been made in computer simulation studies of model biomembranes and other important membrane related structures. We discussed several examples where, in the recent past, large scale atomistic MD techniques have been successfully employed. These studies include highly polyunsaturated lipid bilayers, membrane proteins forming ion-channels, effects of surfactant impurities on biomembranes, and lipid-DNA gene transfer complexes. The results obtained from all these studies were in excellent agreement with experiments. This clearly indicates that MD simulations can provide valuable insights in elucidating the structural, dynamical, and functional properties of such complex systems and can act as powerful complements to real experiments and much less detailed theoretical models. The successes achieved in the past decade indicate that the use of atomistic computer simulations as a means of probing even more complex biological systems will inevitably continue.

ACKNOWLEDGMENTS

This work was supported by generous grants from the National Institutes of Health and the National Science Foundation. Computer resources were provided by NPACI San Diego, CA and PSC Pittsburgh, PA.

REFERENCES

1. *Structure and Dynamics of Membranes* Handbook of Biological Physics, Vol. 1A and 1B (1995) (Lipowsky, R. and Sackmann, E., eds) Elsevier, Amsterdam.
2. Small, D. M. (1986) *The Physical Chemistry of Lipids: From Alkanes to Phospholipids*, Handbook of lipid research, Vol. 4. Plenum Press, New York.

3. *Biological Membranes: A Molecular Perspective from Computation and Experiment* (1996) (Merz, Jr., K. M. and Roux, B., eds), Birkhauser, Boston.
4. Allen, M. P. and Tildesley, D. J. (1987) *Computer Simulation of Liquids*, Clarendon Press, Oxford.
5. Frenkel, D. and Smit, B. (1996) *Understanding Molecular Simulation*, Academic Press, London.
6. Feller, S. E. and Pastor, R. W. (1999) Constant surface tension simulations of lipid bilayers: The sensitivity of surface areas and compressibilities. *J. Chem. Phys.* **111**:1281–1287.
7. Essman, U. and Berkowitz, M. L. (1999) Dynamical properties of phospholipid bilayers from computer simulation. *Biophys. J.* **76**:2081–2089.
8. Damodaran, K. V. and Merz, K. N. (1994) A comparison of DMPC-based and DLPE-based lipid bilayers. *Biophys. J.* **66**:1076–1087.
9. Tieleman, D. P. and Berendsen H. J. C. (1996) Molecular dynamics simulations of a fully hydrated dipalmitoyl phosphatidylcholine bilayer with different macroscopic boundary conditions and parameters. *J. Chem. Phys.* **105**:4871–4880.
10. Tu, K., Tobias, D. J., and Klein, M. L. (1995) Constant pressure and temperature molecular dynamics simulation of a fully hydrated liquid crystal phase dipalmitoylphosphatidylcholine bilayer. *Biophys. J.* **69**:2558–2562.
11. Saiz, L. and Klein, M. L. (2001) Structural properties of a highly polyunsaturated lipid bilayer from molecular dynamics simulations. *Biophys. J.* **81**:204–216.
12. Chiu, S. W., Jakobsson, E., Subramaniam, S., and Scott, H. L. (1999) Combined Monte Carlo and molecular dynamics simulation of fully hydrated dioleyl and palmitoyl-oleyl phosphatidylcholine lipid bilayers. *Biophys. J.* **77**:2462–2469.
13. Pasenkiewicz-Gierula, M. *et al.* (1999) Charge pairing of headgroups in phosphatidylcholine membranes: A molecular dynamics simulation study. *Biophys. J.* **76**:1228–1240.
14. Shinoda, W., Shimizu, M., and Okazaki, S. (1998) Molecular dynamics study on electrostatic properties of a lipid bilayer: Polarization, electrostatic potential, and the effects on structure and dynamics of water near the interface. *J. Phys. Chem. B* **102**:6647–6654.
15. Tobias, D. J. (2001) Electrostatics calculations: recent methodological advances and applications to membranes. *Curr. Op. in Struct. Bio.* **11**:253–261.
16. Forrest, L. R. and Sanson, M. S. P. (2000) Membrane simulations: Bigger and better? *Curr. Op. in Struct. Bio.* **10**:174–181.
17. Feller, S. E. (2000) Molecular dynamics simulations of lipid bilayers. *Curr. Op. Colloid In.* **5**:217–223.
18. Jakobsson, E. (1997) Computer simulation studies of biological membranes: Progress, promise and pitfalls. *Trends Biochem. Sci.* **22**:339–344.
19. Zhong, Q. F., Husslein, T., and Klein, M. L. 1998) Ion channels: A challenge for computer simulations. In: *Classical and Quantum Dynamics in Condensed Phase Simulations* (B. J. Berne, G. Ciccotti, and D. F. Coker, eds). World Scientific, Singapore.
20. Cornell W. D. *et al.* (1995) A second generation force field for the simulation of proteins and nucleic acids. *J. Am. Chem. Soc.* **117**:5179–5197.
21. Brooks, B. R. *et al.* (1983) CHARMM: A program for macromolecular energy, minimization, and dynamics calculations. *J. Comput. Chem.* **4**:187–217.
22. Jorgensen, W. L., Maxwell, D., and Tirado-Rives, J. (1996) Development and testing of the OPLS all-atom force field on conformational energetics and properties of organic liquids. *J. Am. Chem. Soc.* **118**:11225–11236.
23. Berendsen, H. J. C., van der Spoel, D., and van Drunen, R. (1995) GROMACS: A message-passing parallel molecular dynamics implementation. *Comput. Phys. Commun.* **91**:43–56.
24. Feller, S. E., Yin, D., Pastor, R. W., and MacKerell, Jr., A. D. (1997) Molecular dynamics simulation of unsaturated lipids at low hydration: Parametrization and comparison with diffraction studies. *Biophys. J.* **73**:2269–2279.
25. Schlenkrich, M., Brickmann, J., MacKerell, Jr., A. D., and Karplus, M. (1996) An empirical potential energy function for phospholipids: Criteria for parameter optimization and applications. Cited in ref 3, pages 31–82.
26. Feller, S. E. and MacKerell, Jr., A. D. (2000) An improved empirical potential energy function for molecular simulations of phospholipids. *J. Phys. Chem. B* **104**:7510–7515.
27. Foloppe, N. and Tuckerman, M. (1998) Parameter optimization for molecular dynamics simulations. *J. Comput. Chem.* **19**:103–115.
28. MacKerell, Jr., A. D. (1998) Molecular dynamics studies of protein-ligand complexes. *J. Chem. Phys.* **109**:103–115.
29. Jorgensen, W. L. (1998) Molecular dynamics simulations of proteins. *J. Chem. Phys.* **109**:103–115.
30. Darden, T., York, D., and Pedersen, L. (1997) Particle-mesh Ewald: An N log N method for simulating the interaction of a large number of particles. *J. Chem. Phys.* **107**:59–72.
31. Tuckerman, M. (1998) Molecular dynamics simulations. *J. Chem. Phys.* **109**:103–115.
32. Martyna, G. J. and Tuckerman, M. (1998) Integrators for extended systems. *J. Chem. Phys.* **109**:103–115.
33. Martyna, G. J. and Tuckerman, M. (1998) Ensemble via coarse-graining. *J. Chem. Phys.* **109**:103–115.
34. Tuckerman, M. (1998) Molecular dynamics calculations via coarse-graining. *J. Chem. Comput. Phys.* **109**:103–115.
35. Bloom, M., Lin, S., and Tuckerman, M. (1998) The functional role of the lipid bilayer in protein folding. *Approaches from Theory* (Enrico Fermi Lectures, Vol. 16, No. 1), 1–100.
36. Crawford, M. A. (1998) The modern hominid brain. *Science* **280**:1343–1347.
37. Hamilton, J., Cullinan, S., and Phillips, D. (1998) The phosphatidylserine hypothesis. *Science* **280**:1343–1347.
38. Palczewski, K., Kuhn, J., and Tamm, K. (1998) *Science* **280**:739–745.
39. Litman, B. J. and Tamm, K. (1998) Protein function in the phosphatidylserine hypothesis. *Science* **280**:739–745.
40. Bloom, M. (1998) The phosphatidylserine hypothesis. *Science* **280**:739–745.
41. Brown, M. F. and Tamm, K. (1998) *Science* **280**:739–745.
42. de Urquiza, A., Tamm, K., and Tamm, K. (1998) The phosphatidylserine hypothesis. *Science* **280**:739–745.
43. Salmon, A. *et al.* (1998) The phosphatidylserine hypothesis. *Science* **280**:739–745.
44. Barry, J. A., Tamm, K., and Tamm, K. (1998) The phosphatidylserine hypothesis. *Science* **280**:739–745.
45. Huster, D., Jin, S., and Tamm, K. (1998) The phosphatidylserine hypothesis. *Science* **280**:739–745.
46. Olbrich, K., Riedel, K., and Tamm, K. (1998) The phosphatidylserine hypothesis. *Science* **280**:739–745.
47. Koenig, B. W., Tamm, K., and Tamm, K. (1998) The phosphatidylserine hypothesis. *Science* **280**:739–745.
48. Rawicz, W., Tamm, K., and Tamm, K. (1998) The phosphatidylserine hypothesis. *Science* **280**:739–745.
49. Cantor, R. S., Tamm, K., and Tamm, K. (1998) The phosphatidylserine hypothesis. *Science* **280**:739–745.
50. Hyvönen, M., Tamm, K., and Tamm, K. (1998) The phosphatidylserine hypothesis. *Science* **280**:739–745.

andyopadhyay, and Klein
xperiment (1996) (Merz,
Clarendon Press, Oxford.
demic Press, London.
ns of lipid bilayers: The
1287.
olipid bilayers from com-
d and DLPE-based lipid
tions of a fully hydrated
ary conditions and par-
tature molecular dynam-
sphatidylcholine bilayer.
urated lipid bilayer from
bined Monte Carlo and
leyl phosphatidylcholine
osphatidylcholine mem-
s study on electrostatic
effects on structure and
nences and applications to
and better? *Curr. Op. in
Op. Colloid In.* **5**:217–
s: Progress, promise and
nge for computer simu-
ns (B. J. Berne, G. Cic-
n of proteins and nucleic
ergy, minimization, and
and testing of the OPLS
c liquids. *J. Am. Chem.
ACS*: A message-passing
3–56.
olecular dynamics simu-
parison with diffraction
96) An empirical poten-
and applications. Cited
ntial energy function for

27. Foloppe, N. and MacKerell, Jr., A. D. (2000) All-atom empirical force field for nucleic acids: (1) Parameter optimization based on small molecule and condensed phase macro-molecular target data. *J. Comput. Chem.* **21**:86–104.
28. MacKerrell, Jr., A. D. *et al.* (1998) All-atom empirical potential for molecular modeling and dynamics studies of proteins. *J. Phys. Chem. B* **102**:3586–3616.
29. Jorgensen, W. L. *et al.* (1983) Comparison of simple potential functions for simulating liquid water. *J. Chem. Phys.* **79**:926–935.
30. Darden, T., York, D., and Pedersen, L. (1993) Particle mesh Ewald: an $N \log(N)$ method for Ewald sums. *J. Chem. Phys.* **98**:10089–10092.
31. Tuckerman, M. E., Berne, B. J., and Martyna, G. J. (1992) Reversible multiple time scale molecular dynamics. *J. Chem. Phys.* **97**:1990–2001.
32. Martyna, G. J., Tuckerman, M. E., Tobias, D. J., and Klein, M. L. (1996) Explicit reversible integrators for extended system dynamics. *Mol. Phys.* **87**:1117–1157.
33. Martyna, G. J., Klein, M. L., and Tuckerman, M. E. (1992) Nosé-Hoover chains: The canonical ensemble via continuous dynamics. *J. Chem. Phys.* **97**:2635–2643.
34. Tuckerman, M. E. *et al.* (2000) Exploiting multiple levels of parallelism in molecular dynamics based calculations via modern techniques and software paradigms on distributed memory computers. *Comput. Phys. Commun.* **128**:333–376.
35. Bloom, M., Linseisen, F., Lloyd-Smith, J., and Crawford, M. A. (1999) Insights from NMR on the functional role of polyunsaturated lipids in the brain. In: *Magnetic Resonance and Brain Function – Approaches from Physics*, Proceedings of the 1998 Enrico Fermi International School of Physics, Enrico Fermi Lecture, Course #139, Varenna, Italy, ed. B. Maraviglia.
36. Crawford, M. A. *et al.* (1999) Evidence for the unique function of DHA during the evolution of the modern hominid brain. *Lipids* **34**:S39–S47.
37. Hamilton, J., Greiner, R., Salem, N., and Kim, H. Y. (2000) n -3 fatty acid deficiency decreases phosphatidylserine accumulation selectively in neuronal tissues. *Lipids* **35**:863–869 and references therein.
38. Palczewski, K. *et al.* (2000) Crystal structure of rhodopsin: A G protein-coupled receptor. *Science* **289**:739–745.
39. Litman, B. J. and Mitchell, D. C. (1996) A role for polyunsaturation in modulating membrane protein function. *Lipids* **31**:s193–s197.
40. Bloom, M. (1998) Evolution of membranes from a physics perspective. *Biol. Skr. Dan. Vid. Selsk.* **49**:13–17.
41. Brown, M. F. (1994) Modulation of rhodopsin function by properties of the membrane bilayer. *Chem. Phys. Lipids* **73**:159–180.
42. de Urquiza, A. M. *et al.* (2000) Docosahexaenoic acid, ligand for the retinoid X receptor in mouse brain. *Science* **290**:2140–2144.
43. Salmon, A. *et al.* (1987) Configurational statistics of acyl chains in polyunsaturated lipid bilayers from ^2H NMR. *J. Am. Chem. Soc.* **109**:2600–2609.
44. Barry, J. A., Trouard, T. P., Salmon, A., and Brown, M. F. (1991) Low-temperature ^2H NMR spectroscopy of phospholipid bilayers containing docosahexaenoyl (22:6 ω 3) chains. *Biochemistry* **30**:8386–8394.
45. Huster, D., Jin, A. J., Arnold, K., and Gawrisch, K. (1997) Water permeability of polyunsaturated lipid membranes measured by ^{17}O NMR. *Biophys. J.* **73**:855–864.
46. Olbrich, K., Rawicz, W., Needham, D., and Evans, E. (2000) Water permeability of polyunsaturated lipid membranes measured by ^{17}O NMR. *Biophys. J.* **79**:321–327.
47. Koenig, B. W., Strey, H. H., and Gawrisch, K. (1997) Membrane lateral compressibility determined by NMR and X-Ray diffraction: Effect of acyl chain polyunsaturation. *Biophys. J.* **73**:1954–1966.
48. Rawicz, W., Olbrich, K., McIntosh, T., Needham, D., and Evans, E. (2000) Effect of chain length and unsaturation on elasticity of lipid bilayers. *Biophys. J.* **79**:328–339.
49. Cantor, R. S. (1999) Lipid composition and the lateral pressure profile in bilayers. *Biophys. J.* **76**:2625–2639.
50. Hyvönen, M. T., Rantala, T. T., and Ala-Korpela, M. (1997) Structure and dynamic properties of diunsaturated 1-palmitoyl-2-linoleoyl-sn-phosphatidylcholine lipid bilayer from molecular dynamics simulation. *Biophys. J.* **73**:2907–2923.

51. Saiz, L. and Klein, M. L. (2001) Influence of highly polyunsaturated lipid acyl chains of biomembranes on the NMR order parameters. *J. Am. Chem. Soc.* **123**:7381–7387.

52. Saiz, L. and Klein, M. L. (2002) Electrostatic interactions in a neutral model phospholipid bilayer by molecular dynamics simulations. *J. Chem. Phys.* **116**:3052–3057.

53. Rajamoorthi, K. and Brown, M. F. (1991) Bilayers of arachidonic acid containing phospholipids studied by ^2H and ^{31}P NMR spectroscopy. *Biochemistry* **30**:4204–4212.

54. Holte, L. L., Peter, S. A., Sinnwell, T. M., and Gawrisch, K. (1995) ^2H nuclear magnetic resonance order parameter profiles suggest a change of molecular shape for phosphatidylcholines containing a polyunsaturated acyl chain. *Biophys. J.* **68**:2396–2403.

55. Albrand, M., Pageaux, J.-F., Lagarde, M., and Dolmazon, R. (1994) Conformational analysis of isolated docosahexaenoic acid (22:6n-3) and its 14-(S) and 11-(S) hydroxyl derivatives by force field calculations. *Chem. Phys. Lipids* **72**:7–17.

56. Applegate, K. R. and Glomset, J. A. (1986) Computer-based modelling of the conformation and packing properties of docosahexaenoic acid. *J. Lipid Res.* **27**:658–660; Applegate, K. R. and Glomset, J. A. (1991) Effect of acyl chain unsaturation on the conformation of model diacylglycerols: a computer modelling study. *J. Lipid Res.* **32**:1655–1644.

57. Gawrisch, K. (2001) Properties of polyunsaturated lipid membranes. *Biophys. J.* **80**:32A.

58. Parsegian, V. A. and Rand, R. P. (1995) Interactions in membrane assemblies. In Ref. 1, 643–690.

59. Bandyopadhyay, S., Tarek, M., and Klein, M. L. (1999) Molecular dynamics study of a lipid–DNA complex. *J. Phys. Chem. B* **103**:10075–10080.

60. Heerklotz, H. *et al.* (1997) Lipid/detergent interaction thermodynamics as a function of molecular shape. *J. Phys. Chem. B* **101**:639–645.

61. Thurmond, R. L., Otten, D., Brown, M. F., and Beyer, K. (1994) Structure and packing of phosphatidylcholines in lamellar and hexagonal liquid-crystalline mixtures with a nonionic detergent—A wide-line deuterium and P-31 NMR study. *J. Phys. Chem.* **98**:972–983.

62. Otten, D., Löbbecke, L., and Beyer, K. (1995) Stages of the bilayer-micelle transition in the system phosphatidylcholine-C₁₂E₈ as studied by deuterium NMR and phosphorous NMR, light scattering, and calorimetry. *Biophys. J.* **68**:584–597.

63. Levy, D., Gulik, A., Seigneuret, M., and Rigaud, J. L. (1990) Phospholipid vesicle solubilization and reconstruction by detergents—symmetrical analysis of the 2 processes using octaethylene glycol mono-n-dodecyl ether. *Biochemistry* **29**:9480–9488.

64. Klose, G., Islamov, A., König, B., and Cherezov, V. (1996) Structure of mixed multilayers of palmitoleoylphosphatidylcholine and oligo (oxyethylene glycol) monododecyl ether determined by X-ray and neutron diffraction. *Langmuir* **12**:409–415.

65. Klose, G., Mädler, B., Shäfer, H., and Schneider, K. P. (1999) Structural characterization of POPC, and C₁₂E₄ in their mixed membranes at reduced hydration by solid state ^2H NMR. *J. Phys. Chem. B* **103**:3022–3029.

66. Schmiedel, H., Jorchem, P., Kiselev, M., and Klose, G. (2001) Determination of structural parameters and hydration of unilamellar POPC/C₁₂E₄ vesicles at high water excess from neutron scattering curves using a novel method of evaluation. *J. Phys. Chem. B* **105**:111–117.

67. Meijer, L. A., Leermakers, F. A. M., and Lyklema, J. (1999) Self-consistent-field modeling of complex molecules with united atom detail in inhomogeneous systems. Cyclic and branched foreign molecules in dimyristoylphosphatidylcholine membranes. *J. Chem. Phys.* **110**:6560–6579.

68. König, B., Dietrich, U., and Klose, G. (1997) Hydration and structural properties of mixed lipid/surfactant model membranes. *Langmuir* **13**:525–532.

69. Klose, G. and Levine, Y. K. (2000) Membranes of palmitoylpleyleylphosphatidylcholine and C₁₂E₄—A lattice model simulation. *Langmuir* **16**:671–676.

70. Bandyopadhyay, S., Shelley, J. C., and Klein, M. L. (2000) Molecular dynamics study of the effect of surfactant on a biomembrane. *J. Phys. Chem. B* **105**:5979–5986.

71. Schneider, M. J. and Feller, S. E. (2001) Molecular dynamics simulations of a phospholipid-detergent mixture. *J. Phys. Chem. B* **105**:1331–1337.

72. Hille, B. (1992) Ionic channels of excitable membranes. Sinauer, Sunderland, MA.

73. Doyle, D. A. *et al.* (1998) The structure of the potassium channel: Molecular basis of K⁺ conduction and selectivity. *Science* **280**:69–77.

74. Morais-Cabral, J. B. (1999) The K⁺ conduction rate by the K_{ATP} channel. *Science* **285**:137–138.

75. Zhou, Y., Morais-Cabral, J. B., and MacKinnon, R. (1998) Structure and function of a K⁺ channel. *Nature* **394**:45–48.

76. Bernèche, S., and MacKinnon, R. (1999) Structure of the K⁺ channel. *Nature* **400**:73–77.

77. Oiki, S., Danh, T. T., and MacKinnon, R. (1999) Structure of the ionic channel. *Nature* **400**:77–78.

78. Unwin, N. (1999) Structure of the K⁺ channel. *Nature* **400**:78–79.

79. Changeux, J. P. (1999) Structure of the K⁺ channel. *Nature* **400**:79–80.

80. Chang, G., Spitzer, J. C., and MacKinnon, R. (1999) Structure of the K⁺ channel. *Nature* **400**:80–81.

81. Lear, J. D., Wimley, W. C., and MacKinnon, R. (1999) Structure of the K⁺ channel. *Nature* **400**:81–82.

82. Duff, K. C. and MacKinnon, R. (1999) Structure of the K⁺ channel. *Nature* **400**:82–83.

83. Montal, M. (1999) Structure of the K⁺ channel. *Nature* **400**:83–84.

84. Opella, S. J. *et al.* (1999) Structure of the K⁺ channel. *Nature* **400**:84–85.

85. Zhong, Q. F., and MacKinnon, R. (1999) Structure of the K⁺ channel. *Nature* **400**:85–86.

86. Zhong, Q. F., and MacKinnon, R. (1999) Structure of the K⁺ channel. *Nature* **400**:86–87.

87. Forrest, L. R., and MacKinnon, R. (1999) Structure of the K⁺ channel. *Nature* **400**:87–88.

88. Law, R. J., and MacKinnon, R. (1999) Structure of the K⁺ channel. *Nature* **400**:88–89.

89. Saiz, L. and Klein, M. L. (1999) Structure of the K⁺ channel. *Nature* **400**:89–90.

90. Anderson, O. J., and MacKinnon, R. (1999) Structure of the K⁺ channel. *Nature* **400**:90–91.

91. Woolf, T. B., and MacKinnon, R. (1999) Structure of the K⁺ channel. *Nature* **400**:91–92.

92. Roux, B., and MacKinnon, R. (1999) Structure of the K⁺ channel. *Nature* **400**:92–93.

93. de Planque, M., and MacKinnon, R. (1999) Structure of the K⁺ channel. *Nature* **400**:93–94.

94. Zein, M., and MacKinnon, R. (1999) Structure of the K⁺ channel. *Nature* **400**:94–95.

95. Paré, C., *et al.* (1999) Structure of the K⁺ channel. *Nature* **400**:95–96.

96. Roux, B., and MacKinnon, R. (1999) Structure of the K⁺ channel. *Nature* **400**:96–97.

97. Saiz, L., and MacKinnon, R. (1999) Structure of the K⁺ channel. *Nature* **400**:97–98.

98. Singhal, A., and MacKinnon, R. (1999) Structure of the K⁺ channel. *Nature* **400**:98–99.

99. Mulligan, R., and MacKinnon, R. (1999) Structure of the K⁺ channel. *Nature* **400**:99–100.

100. Miller, A. D., and MacKinnon, R. (1999) Structure of the K⁺ channel. *Nature* **400**:100–101.

Bandyopadhyay, and Klein
d acyl chains of biomem-
odel phospholipid bilayer
containing phospholipids
uclear magnetic resonance
atidylcholines containing
nformational analysis of
derivatives by force field
of the conformation and
plegate, K. R. and Glom-
model diacylglycerols: a
phys. J. **80**:32A.
bles. In Ref. 1, 643–690.
ics study of a lipid–DNA
is a function of molecular
ure and packing of phos-
h a nonionic detergent—
B.
e transition in the system
us NMR, light scattering,
ipid vesicle solubilization
using octaethylene glycol
ixed multilayers of palmi-
l ether determined by X-
haracterization of POPC,
H NMR. *J. Phys. Chem.*
n of structural parameters
from neutron scattering
nt-field modeling of com-
lic and branched foreign
110:6560–6579.
roperties of mixed lipid/
atidylcholine and C₁₂E₄—
nematics study of the effect
of a phospholipid-deter-
nd, MA.
ar basis of K⁺ conduction

74. Morais-Cabral, J. H., Zhou, Y., and Mackinnon, R. (2001) Energetic optimization of ion conduction rate by the K⁺ selectivity filter. *Science* **414**:37–42.
75. Zhou, Y., Morais-Cabral, J. H., Kaufman, A., and Mackinnon, R. (2001) Chemistry of ion coordination and hydration revealed by a K⁺ channel-Fab complex at 2.0 Å resolution. *Science* **414**:43–48.
76. Bernèche, S., and Roux, B. (2001) Energetics of ion conduction through the K⁺ channel. *Science* **414**:73–77.
77. Oiki, S., Danho, W., Madison, V., and Montal, M. (1988) M2- δ , a candidate for the structure lining the ionic channel of the nicotinic cholinergic receptor. *Proc. Natl. Acad. Sci. USA* **85**:8703–8707.
78. Unwin, N. (1995) Acetylcholine-receptor channel imaged in the open state. *Nature* **373**:37–43.
79. Changeux, J. P. (1993) Chemical signalling in the brain. *Scienc. Amer.* **1**:58–62.
80. Chang, G., Spencer, R. H., Lee, A. T., Barclay, M. T., and Rees, D. C. (1998) Structure of the MscL homolog from mycobacterium tuberculosis: a gated mechanosensitive ion channel. *Science* **282**:2220–2226.
81. Lear, J. D., Wasserman, Z. R., and DeGrado, W. F. (1988) Synthetic amphiphilic peptide models for protein ion channels. *Science* **240**:1177–1181.
82. Duff, K. C. and Ashley, R. H. (1992) The transmembrane domain of influenza-A M2 protein forms adamantine-sensitive proton channels in planar lipid bilayers. *Virology* **190**:485–489.
83. Montal, M. (1995) Design of molecular function—Channels of communication. *Annu. Rev. Biophys. Biomol. Struct.* **24**:31–57.
84. Opella, S. J. *et al.* (1999) Structures of the M2 channel-lining segments from nicotinic acetylcholine and NMDA receptors by NMR spectroscopy. *Nature Struct. Biol.* **6**:374–379.
85. Zhong, Q. F. *et al.* (1998) Molecular dynamics simulation of a synthetic ion channel. *Biophys. J.* **74**:3–10.
86. Zhong, Q. F. *et al.* (1998) The M2 channel of influenza A virus: a molecular dynamics study. *FEBS Lett.* **434**:265–271.
87. Forrest, L. R. *et al.* (2000) Exploring models of the influenza A M2 channel: MD simulations in a phospholipid bilayer. *Biophys. J.* **78**:55–69.
88. Law, R. J. *et al.* (2000) Structure and dynamics of the pore-lining helix of the nicotinic receptor: MD simulations in water, lipid bilayers, and transbilayer bundles. *Proteins* **39**:47–55.
89. Saiz, L. and Klein, M. L. (2001) Structure of the pore region of the nicotinic acetylcholine receptor ion channel: A molecular dynamics simulation study (*preprint*).
90. Anderson, O. S. *et al.* (1998) Gramicidin channels: Molecular force transducers in lipid bilayers. *Biol. Skr. Dan. Vid. Selsk.* **49**:75–82.
91. Woolf, T. B. and Roux, B. (1994) Molecular dynamics simulation of the gramicidin channel in a phospholipid bilayer. *Proc. Natl. Acad. Sci. USA* **91**:11631–11635.
92. Roux, B. and Karplus, M. (1994) Molecular dynamics simulation of the gramicidin channel. *Ann. Rev. Biophys. Biomol. Struct.* **23**:731–761.
93. de Planque, M. R. *et al.* (1998) Influence of lipid/peptide hydrophobic mismatch on the thickness of diacylphosphatidylcholine bilayers. A ²H NMR and ESR study using designed transmembrane α -helical peptides and gramicidin A. *Biochemistry* **37**:9333–9345.
94. Zein, M. and Winter, R. (2000) Effect of temperature, pressure, and lipid acyl chain length on the structure and phase behaviors of phospholipid-gramicidin bilayers. *Phys. Chem. Phys.* **2**:4545–4551.
95. Paré C. *et al.* (2001) Differential scanning calorimetry and ²H nuclear magnetic resonance and Fourier transform infrared spectroscopy studies of the effects of transmembrane α -helical peptides on the organization of phosphocholine bilayers. *Biochim. Biophys. Acta* **1511**:60–73.
96. Roux, M. *et al.* (1989) Conformational changes of phospholipid headgroups induced by a cationic integral membrane peptide as seen by deuterium magnetic resonance. *Biochemistry* **28**:2313–2321.
97. Saiz, L., Bandyopadhyay, S., and Klein, M. L. (2002) Influence of an homopentameric bundle of transmembrane α -helical peptides forming the pore region of an ion channel on the physical properties of a phospholipid layer (*unpublished*).
98. Singhal, A. and Huang, L. (1994) *Gene Therapeutics: Methods and Applications of Direct Gene Transfer*. Birkhauser: Boston.
99. Mulligan, R. (1993) The basic science of gene therapy. *Science* **260**:926–932.
100. Miller, A. D. (1992) Human gene therapy comes of age. *Nature* **357**:445–460.

101. Safinya, C. R. and Addadi, L. (1996) Biomaterials. *Curr. Opin. in Solid State and Mat. Sci.* **1**:387–391.
102. Crystal, R. G. (1995) Transfer of genes to humans: early lessons and obstacles to success. *Science* **270**:404–410.
103. Felgner, P. L. *et al.* (1987) Lipofection: a highly efficient, lipid-mediated DNA-transfection procedure. *Proc. Natl. Acad. Sci. USA* **84**:7413–7417.
104. Rädler, J. O., Koltover, I., Salditt, T., and Safinya, C. R. (1997) Structure of DNA -cationic liposome complexes: DNA intercalation in multilamellar membranes in distinct interhelical packing regimes. *Science* **275**:810–814.
105. Salditt, T., Koltover, I., Rädler, J. O., and Safinya, C. R. (1997) Two-dimensional smectic ordering of linear DNA chains in self-assembled DNA-cationic liposome mixtures. *Phys. Rev. Lett.* **79**:2582–2585.
106. Artzner, F., Zantl, R., Rapp, G., and Rädler, J. O. (1998) Observations of a rectangular columnar phase in condensed lamellar cationic lipid–DNA complexes. *Phys. Rev. Lett.* **81**:5015–5018.
107. Zantl, R., Artzner, F., Rapp, G., and Rädler, J. O. (1999) Thermotropic structural changes of saturated-cationic-lipid–DNA complexes. *Europhys. Lett.* **45**:90–96.
108. Zantl, R. *et al.* (1999) Thermotropic phase behavior of cationic lipid–DNA complexes compared to binary lipid mixtures. *J. Phys. Chem. B* **103**:10300–10310.
109. Koltover, I., Salditt, T., Rädler, J. O., and Safinya, C. R. (1998) An inverted hexagonal phase of cationic liposome–DNA complexes related to DNA release and delivery. *Science* **281**:78–81.
110. Rädler, J. O. *et al.* (1998) Structure and Interfacial aspects of self-assembled cationic lipid–DNA gene carrier complexes. *Lamgnuir* **14**:4272–4283.
111. O'Hern, C. S. and Lubensky, T. C. (1998) Sliding columnar phase of DNA-lipid complex. *Phys. Rev. Lett.* **80**:4345–4348.
112. Golubovic, L. and Golubovic, M. (1998) Fluctuations of quasi-two-dimensional smectics intercalated between membranes in multilamellar phases of DNA-cationic lipid complexes. *Phys. Rev. Lett.* **80**:4341–4344.
113. Harries, D., May, S., Gelbart, W. M., and Ben-Shaul, A. (1998) Structure, stability, and thermodynamics of lamellar DNA-lipid complexes. *Biophys. J.* **75**:159–173.
114. Bruinsma, R. (1998) Electrostatics of DNA cationic lipid complexes: isoelectric instability. *Euro. Phys. J. B* **4**:75–88.
115. Dan, N. (1997) Multilamellar structures of DNA complexes with cationic liposomes. *Biophys. J.* **73**:1842–1846.
116. Felgner, P. L. and Rhodes, G. (1991) Gene therapeutics. *Nature* **349**:351–352.
117. Höltje, M. *et al.* (2001) Molecular dynamics simulations of stratum corneum lipid models: fatty acids and cholesterol. *Biochim. Biophys. Acta* **1511**:156–167.
118. Edholm, O. and Nyberg, A. M. (1992) Cholesterol in model membranes: A molecular-dynamics simulation. *Biophys. J.* **63**:1081–1089.
119. Gabdoulline, R. R., Vanderkooi, G., and Zheng, C. (1996) Comparison of the structures of dimyristoylphosphatidylcholine in the presence and absence of cholesterol by molecular dynamics simulations. *J. Phys. Chem.* **100**:15942–15946.
120. Robinson, A. J., Richards, W. G., Thomas, P. J., and Hann, M. M. (1995) Behavior of cholesterol and its effect on head group and chain conformations in lipid bilayers: A molecular-dynamics study. *Biophys. J.* **68**:164–170.
121. Tu, K. C., Klein, M. L., and Tobias, D. J. (1998) Constant-pressure molecular dynamics investigation of cholesterol effects in a dipalmitoylphosphatidylcholine bilayer. *Biophys. J.* **75**:2147–2156.
122. Smondyrev, A. M. and Berkowitz, M. L. (1999) Structure of dipalmitoylphosphatidylcholine/cholesterol bilayer at low and high cholesterol concentrations: Molecular dynamics simulation. *Biophys. J.* **77**:2075–2089.
123. Paseniewicz-Gierula, M., Rog, T., Kitamura, K., and Kusumi, A. (2000) Cholesterol effects on the phosphatidylcholine bilayer polar region: A molecular simulation study. *Biophys. J.* **78**:1376–1389.
124. Chiu, S. W., Jakobsson, E., and Scott, H. L. (2001) Combined Monte Carlo and molecular dynamics simulation of hydrated lipid–cholesterol lipid bilayers at low cholesterol concentration. *Biophys. J.* **80**:1104–1114.
125. Brown, D. A. and Goetz, R. (1998) Cholesterol in membranes. *Mol. Membr. Biol.* **15**:1–12.
126. Simons, K. and Siegel, M. (1999) Cholesterol in human bile. *Biochim. Biophys. Acta* **1469**:8352.
127. Marrink, S. J. and Lindahl, E. (1999) Effect of melittin at the lipid–water interface. *Biophys. J.* **77**:105–114.
128. Hristova, K., Lindahl, E., and Marrink, S. J. (1999) Effect of melittin at the lipid–water interface. *Biophys. J.* **77**:105–114.
129. Huang, H. W. and Marrink, S. J. (1999) Effect of melittin at the lipid–water interface. *Biophys. J.* **77**:105–114.
130. Popot, J.-L. and Engelman, B. M. (1999) A two-stage model. *Biophys. J.* **77**:115–124.
131. White, S. H. and Engelman, B. M. (1999) *Annu. Rev. Biochem.* **68**:633–674.
132. Marrink, S. J. and Lindahl, E. (1999) Aggregation of phospholipids. *Biophys. J.* **77**:125–134.
133. Lindahl, E. and Engelman, B. M. (1999) Lipid bilayers and membranes. *Biophys. J.* **77**:135–144.
134. Shelley, J. C. and Engelman, B. M. (1999) *J. Phys. Chem. B* **103**:4464–4470.
135. Goetz, R., Goetz, R., and Marrink, S. J. (1999) Cholesterol in lipid bilayers. *Biophys. J.* **77**:145–154.
136. Marrink, S. J. and Lindahl, E. (1999) Cholesterol in lipid bilayers. *Biophys. J.* **77**:145–154.
137. Lindahl, E. and Marrink, S. J. (1999) Cholesterol in lipid bilayers. *Biophys. J.* **77**:145–154.
138. Nagle, J. F. and Helfman, D. M. (1999) *J. Phys. Chem. B* **103**:4471–4478.
139. Marrink, S. J. and Lindahl, E. (1999) Cholesterol in lipid bilayers. *Biophys. J.* **77**:145–154.
140. Marrink, S. J. and Lindahl, E. (1999) Cholesterol in lipid bilayers. *Biophys. J.* **77**:145–154.
141. Marrink, S. J. and Lindahl, E. (1999) Cholesterol in lipid bilayers. *Biophys. J.* **77**:145–154.
142. Marrink, S. J. and Lindahl, E. (1999) Cholesterol in lipid bilayers. *Biophys. J.* **77**:145–154.
143. Marrink, S. J. and Lindahl, E. (1999) Cholesterol in lipid bilayers. *Biophys. J.* **77**:145–154.
144. Marrink, S. J. and Lindahl, E. (1999) Cholesterol in lipid bilayers. *Biophys. J.* **77**:145–154.
145. Marrink, S. J. and Lindahl, E. (1999) Cholesterol in lipid bilayers. *Biophys. J.* **77**:145–154.
146. Marrink, S. J. and Lindahl, E. (1999) Cholesterol in lipid bilayers. *Biophys. J.* **77**:145–154.
147. Marrink, S. J. and Lindahl, E. (1999) Cholesterol in lipid bilayers. *Biophys. J.* **77**:145–154.
148. Marrink, S. J. and Lindahl, E. (1999) Cholesterol in lipid bilayers. *Biophys. J.* **77**:145–154.
149. Marrink, S. J. and Lindahl, E. (1999) Cholesterol in lipid bilayers. *Biophys. J.* **77**:145–154.
150. Marrink, S. J. and Lindahl, E. (1999) Cholesterol in lipid bilayers. *Biophys. J.* **77**:145–154.
151. Marrink, S. J. and Lindahl, E. (1999) Cholesterol in lipid bilayers. *Biophys. J.* **77**:145–154.
152. Marrink, S. J. and Lindahl, E. (1999) Cholesterol in lipid bilayers. *Biophys. J.* **77**:145–154.
153. Marrink, S. J. and Lindahl, E. (1999) Cholesterol in lipid bilayers. *Biophys. J.* **77**:145–154.
154. Marrink, S. J. and Lindahl, E. (1999) Cholesterol in lipid bilayers. *Biophys. J.* **77**:145–154.
155. Marrink, S. J. and Lindahl, E. (1999) Cholesterol in lipid bilayers. *Biophys. J.* **77**:145–154.
156. Marrink, S. J. and Lindahl, E. (1999) Cholesterol in lipid bilayers. *Biophys. J.* **77**:145–154.
157. Marrink, S. J. and Lindahl, E. (1999) Cholesterol in lipid bilayers. *Biophys. J.* **77**:145–154.
158. Marrink, S. J. and Lindahl, E. (1999) Cholesterol in lipid bilayers. *Biophys. J.* **77**:145–154.
159. Marrink, S. J. and Lindahl, E. (1999) Cholesterol in lipid bilayers. *Biophys. J.* **77**:145–154.
160. Marrink, S. J. and Lindahl, E. (1999) Cholesterol in lipid bilayers. *Biophys. J.* **77**:145–154.
161. Marrink, S. J. and Lindahl, E. (1999) Cholesterol in lipid bilayers. *Biophys. J.* **77**:145–154.
162. Marrink, S. J. and Lindahl, E. (1999) Cholesterol in lipid bilayers. *Biophys. J.* **77**:145–154.
163. Marrink, S. J. and Lindahl, E. (1999) Cholesterol in lipid bilayers. *Biophys. J.* **77**:145–154.
164. Marrink, S. J. and Lindahl, E. (1999) Cholesterol in lipid bilayers. *Biophys. J.* **77**:145–154.
165. Marrink, S. J. and Lindahl, E. (1999) Cholesterol in lipid bilayers. *Biophys. J.* **77**:145–154.
166. Marrink, S. J. and Lindahl, E. (1999) Cholesterol in lipid bilayers. *Biophys. J.* **77**:145–154.
167. Marrink, S. J. and Lindahl, E. (1999) Cholesterol in lipid bilayers. *Biophys. J.* **77**:145–154.
168. Marrink, S. J. and Lindahl, E. (1999) Cholesterol in lipid bilayers. *Biophys. J.* **77**:145–154.
169. Marrink, S. J. and Lindahl, E. (1999) Cholesterol in lipid bilayers. *Biophys. J.* **77**:145–154.
170. Marrink, S. J. and Lindahl, E. (1999) Cholesterol in lipid bilayers. *Biophys. J.* **77**:145–154.
171. Marrink, S. J. and Lindahl, E. (1999) Cholesterol in lipid bilayers. *Biophys. J.* **77**:145–154.
172. Marrink, S. J. and Lindahl, E. (1999) Cholesterol in lipid bilayers. *Biophys. J.* **77**:145–154.
173. Marrink, S. J. and Lindahl, E. (1999) Cholesterol in lipid bilayers. *Biophys. J.* **77**:145–154.
174. Marrink, S. J. and Lindahl, E. (1999) Cholesterol in lipid bilayers. *Biophys. J.* **77**:145–154.
175. Marrink, S. J. and Lindahl, E. (1999) Cholesterol in lipid bilayers. *Biophys. J.* **77**:145–154.
176. Marrink, S. J. and Lindahl, E. (1999) Cholesterol in lipid bilayers. *Biophys. J.* **77**:145–154.
177. Marrink, S. J. and Lindahl, E. (1999) Cholesterol in lipid bilayers. *Biophys. J.* **77**:145–154.
178. Marrink, S. J. and Lindahl, E. (1999) Cholesterol in lipid bilayers. *Biophys. J.* **77**:145–154.
179. Marrink, S. J. and Lindahl, E. (1999) Cholesterol in lipid bilayers. *Biophys. J.* **77**:145–154.
180. Marrink, S. J. and Lindahl, E. (1999) Cholesterol in lipid bilayers. *Biophys. J.* **77**:145–154.
181. Marrink, S. J. and Lindahl, E. (1999) Cholesterol in lipid bilayers. *Biophys. J.* **77**:145–154.
182. Marrink, S. J. and Lindahl, E. (1999) Cholesterol in lipid bilayers. *Biophys. J.* **77**:145–154.
183. Marrink, S. J. and Lindahl, E. (1999) Cholesterol in lipid bilayers. *Biophys. J.* **77**:145–154.
184. Marrink, S. J. and Lindahl, E. (1999) Cholesterol in lipid bilayers. *Biophys. J.* **77**:145–154.
185. Marrink, S. J. and Lindahl, E. (1999) Cholesterol in lipid bilayers. *Biophys. J.* **77**:145–154.
186. Marrink, S. J. and Lindahl, E. (1999) Cholesterol in lipid bilayers. *Biophys. J.* **77**:145–154.
187. Marrink, S. J. and Lindahl, E. (1999) Cholesterol in lipid bilayers. *Biophys. J.* **77**:145–154.
188. Marrink, S. J. and Lindahl, E. (1999) Cholesterol in lipid bilayers. *Biophys. J.* **77**:145–154.
189. Marrink, S. J. and Lindahl, E. (1999) Cholesterol in lipid bilayers. *Biophys. J.* **77**:145–154.
190. Marrink, S. J. and Lindahl, E. (1999) Cholesterol in lipid bilayers. *Biophys. J.* **77**:145–154.
191. Marrink, S. J. and Lindahl, E. (1999) Cholesterol in lipid bilayers. *Biophys. J.* **77**:145–154.
192. Marrink, S. J. and Lindahl, E. (1999) Cholesterol in lipid bilayers. *Biophys. J.* **77**:145–154.
193. Marrink, S. J. and Lindahl, E. (1999) Cholesterol in lipid bilayers. *Biophys. J.* **77**:145–154.
194. Marrink, S. J. and Lindahl, E. (1999) Cholesterol in lipid bilayers. *Biophys. J.* **77**:145–154.
195. Marrink, S. J. and Lindahl, E. (1999) Cholesterol in lipid bilayers. *Biophys. J.* **77**:145–154.
196. Marrink, S. J. and Lindahl, E. (1999) Cholesterol in lipid bilayers. *Biophys. J.* **77**:145–154.
197. Marrink, S. J. and Lindahl, E. (1999) Cholesterol in lipid bilayers. *Biophys. J.* **77**:145–154.
198. Marrink, S. J. and Lindahl, E. (1999) Cholesterol in lipid bilayers. *Biophys. J.* **77**:145–154.
199. Marrink, S. J. and Lindahl, E. (1999) Cholesterol in lipid bilayers. *Biophys. J.* **77**:145–154.
200. Marrink, S. J. and Lindahl, E. (1999) Cholesterol in lipid bilayers. *Biophys. J.* **77**:145–154.
201. Marrink, S. J. and Lindahl, E. (1999) Cholesterol in lipid bilayers. *Biophys. J.* **77**:145–154.
202. Marrink, S. J. and Lindahl, E. (1999) Cholesterol in lipid bilayers. *Biophys. J.* **77**:145–154.
203. Marrink, S. J. and Lindahl, E. (1999) Cholesterol in lipid bilayers. *Biophys. J.* **77**:145–154.
204. Marrink, S. J. and Lindahl, E. (1999) Cholesterol in lipid bilayers. *Biophys. J.* **77**:145–154.
205. Marrink, S. J. and Lindahl, E. (1999) Cholesterol in lipid bilayers. *Biophys. J.* **77**:145–154.
206. Marrink, S. J. and Lindahl, E. (1999) Cholesterol in lipid bilayers. *Biophys. J.* **77**:145–154.
207. Marrink, S. J. and Lindahl, E. (1999) Cholesterol in lipid bilayers. *Biophys. J.* **77**:145–154.
208. Marrink, S. J. and Lindahl, E. (1999) Cholesterol in lipid bilayers. *Biophys. J.* **77**:145–154.
209. Marrink, S. J. and Lindahl, E. (1999) Cholesterol in lipid bilayers. *Biophys. J.* **77**:145–154.
210. Marrink, S. J. and Lindahl, E. (1999) Cholesterol in lipid bilayers. *Biophys. J.* **77**:145–154.
211. Marrink, S. J. and Lindahl, E. (1999) Cholesterol in lipid bilayers. *Biophys. J.* **77**:145–154.
212. Marrink, S. J. and Lindahl, E. (1999) Cholesterol in lipid bilayers. *Biophys. J.* **77**:145–154.
213. Marrink, S. J. and Lindahl, E. (1999) Cholesterol in lipid bilayers. *Biophys. J.* **77**:145–154.
214. Marrink, S. J. and Lindahl, E. (1999) Cholesterol in lipid bilayers. *Biophys. J.* **77**:145–154.
215. Marrink, S. J. and Lindahl, E. (1999) Cholesterol in lipid bilayers. *Biophys. J.* **77**:145–154.
216. Marrink, S. J. and Lindahl, E. (1999) Cholesterol in lipid bilayers. *Biophys. J.* **77**:145–154.
217. Marrink, S. J. and Lindahl, E. (1999) Cholesterol in lipid bilayers. *Biophys. J.* **77**:145–154.
218. Marrink, S. J. and Lindahl, E. (1999) Cholesterol in lipid bilayers. *Biophys. J.* **77**:145–154.
219. Marrink, S. J. and Lindahl, E. (1999) Cholesterol in lipid bilayers. *Biophys. J.* **77**:145–154.
220. Marrink, S. J. and Lindahl, E. (1999) Cholesterol in lipid bilayers. *Biophys. J.* **77**:145–154.
221. Marrink, S. J. and Lindahl, E. (1999) Cholesterol in lipid bilayers. *Biophys. J.* **77**:145–154.
222. Marrink, S. J. and Lindahl, E. (1999) Cholesterol in lipid bilayers. *Biophys. J.* **77**:145–154.
223. Marrink, S. J. and Lindahl, E. (1999) Cholesterol in lipid bilayers. *Biophys. J.* **77**:145–154.
224. Marrink, S. J. and Lindahl, E. (1999) Cholesterol in lipid bilayers. *Biophys. J.* **77**:145–154.
225. Marrink, S. J. and Lindahl, E. (1999) Cholesterol in lipid bilayers. *Biophys. J.* **77**:145–154.
226. Marrink, S. J. and Lindahl, E. (1999) Cholesterol in lipid bilayers. *Biophys. J.* **77**:145–154.
227. Marrink, S. J. and Lindahl, E. (1999) Cholesterol in lipid bilayers. *Biophys. J.* **77**:145–154.
228. Marrink, S. J. and Lindahl, E. (1999) Cholesterol in lipid bilayers. *Biophys. J.* **77**:145–154.
229. Marrink, S. J. and Lindahl, E. (1999) Cholesterol in lipid bilayers. *Biophys. J.* **77**:145–154.
230. Marrink, S. J. and Lindahl, E. (1999) Cholesterol in lipid bilayers. *Biophys. J.* **77**:145–154.
231. Marrink, S. J. and Lindahl, E. (1999) Cholesterol in lipid bilayers. *Biophys. J.* **77**:145–154.
232. Marrink, S. J. and Lindahl, E. (1999) Cholesterol in lipid bilayers. *Biophys. J.* **77**:145–154.
233. Marrink, S. J. and Lindahl, E. (1999) Cholesterol in lipid bilayers. *Biophys. J.* **77**:145–154.
234. Marrink, S. J. and Lindahl, E. (1999) Cholesterol in lipid bilayers. *Biophys. J.* **77**:145–154.
235. Marrink, S. J. and Lindahl, E. (1999) Cholesterol in lipid bilayers. *Biophys. J.* **77**:145–154.
236. Marrink, S. J. and Lindahl, E. (1999) Cholesterol in lipid bilayers. *Biophys. J.* **77**:145–154.
237. Marrink, S. J. and Lindahl, E. (1999) Cholesterol in lipid bilayers. *Biophys. J.* **77**:145–154.
238. Marrink, S. J. and Lindahl, E. (1999) Cholesterol in lipid bilayers. *Biophys. J.* **77**:145–154.
239. Marrink, S. J. and Lindahl, E. (1999) Cholesterol in lipid bilayers. *Biophys. J.* **77**:145–154.
240. Marrink, S. J. and Lindahl, E. (1999) Cholesterol in lipid bilayers. *Biophys. J.* **77**:145–154.
241. Marrink, S. J. and Lindahl, E. (1999) Cholesterol in lipid bilayers. *Biophys. J.* **77**:145–154.
242. Marrink, S. J. and Lindahl, E. (1999) Cholesterol in lipid bilayers. *Biophys. J.* **77**:145–154.
243. Marrink, S. J. and Lindahl, E. (1999) Cholesterol in lipid bilayers. *Biophys. J.* **77**:145–154.
244. Marrink, S. J. and Lindahl, E. (1999) Cholesterol in lipid bilayers. *Biophys. J.* **77**:145–154.
245. Marrink, S. J. and Lindahl, E. (1999) Cholesterol in lipid bilayers. *Biophys. J.* **77**:145–154.
246. Marrink, S. J. and Lindahl, E. (1999) Cholesterol in lipid bilayers. *Biophys. J.* **77**:145–154.
247. Marrink, S. J. and Lindahl, E. (1999) Cholesterol in lipid bilayers. *Biophys. J.* **77**:145–154.
248. Marrink, S. J. and Lindahl, E. (1999) Cholesterol in lipid bilayers. *Biophys. J.* **77**:145–154.
249. Marrink, S. J. and Lindahl, E. (1999) Cholesterol in lipid bilayers. *Biophys. J.* **77**:145–154.
250. Marrink, S. J. and Lindahl, E. (1999) Cholesterol in lipid bilayers. *Biophys. J.* **77**:145–154.
251. Marrink, S. J. and Lindahl, E. (1999) Cholesterol in lipid bilayers. *Biophys. J.* **77**:145–154.
252. Marrink, S. J. and Lindahl, E. (1999) Cholesterol in lipid bilayers. *Biophys. J.* **77**:145–154.
253. Marrink, S. J. and Lindahl, E. (1999) Cholesterol in lipid bilayers. *Biophys. J.* **77**:145–154.
254. Marrink, S. J. and Lindahl, E. (1999) Cholesterol in lipid bilayers. *Biophys. J.* **77**:145–154.
255. Marrink, S. J. and Lindahl, E. (1999) Cholesterol in lipid bilayers. *Biophys. J.* **77**:145–154.
256. Marrink, S. J. and Lindahl, E. (1999) Cholesterol in lipid bilayers. *Biophys. J.* **77**:145–154.
257. Marrink, S. J. and Lindahl, E. (1999) Cholesterol in lipid bilayers. *Biophys. J.* **77**:145–154.
258. Marrink, S. J. and Lindahl, E. (1999) Cholesterol in lipid bilayers. *Biophys. J.* **77**:145–154.
259. Marrink, S. J. and Lindahl, E. (1999) Cholesterol in lipid bilayers. *Biophys. J.* **77**:145–154.
260. Marrink, S. J. and Lindahl, E. (1999) Cholesterol in lipid bilayers. *Biophys. J.* **77**:145–154.
261. Marrink, S. J. and Lindahl, E. (1999) Cholesterol in lipid bilayers. *Biophys. J.* **77**:145–154.
262. Marrink, S. J. and Lindahl, E. (1999) Cholesterol in lipid bilayers. *Biophys. J.* **77**:145–154.
263. Marrink, S. J. and Lindahl, E. (1999) Cholesterol in lipid bilayers. *Biophys. J.* **77**:145–154.
264. Marrink, S. J. and Lindahl, E. (1999) Cholesterol in lipid bilayers. *Biophys. J.* **77**:145–154.
265. Marrink, S. J. and Lindahl, E. (1999) Cholesterol in lipid bilayers. *Biophys. J.* **77**:145–154.
266. Marrink, S. J. and Lindahl, E. (1999) Cholesterol in lipid bilayers. *Biophys. J.* **77**:145–154.
267. Marrink, S. J. and Lindahl, E. (1999) Cholesterol in lipid bilayers. *Biophys. J.* **77**:145–154.
268. Marrink, S. J. and Lindahl, E. (1999) Cholesterol in lipid bilayers. *Biophys. J.* **77**:145–154.
269. Marrink, S. J. and Lindahl, E. (1999) Cholesterol in lipid bilayers. *Biophys. J.* **77**:145–154.
270. Marrink, S. J. and Lindahl, E. (1999) Cholesterol in lipid bilayers. *Biophys. J.* **77**:145–154.
271. Marrink, S. J. and Lindahl, E. (1999) Cholesterol in lipid bilayers. *Biophys. J.* **77**:145–154.
272. Marrink, S. J. and Lindahl, E. (1999) Cholesterol in lipid bilayers. *Biophys. J.* **77**:145–154.
273. Marrink, S. J. and Lindahl, E. (1999) Cholesterol in lipid bilayers. *Biophys. J.* **77**:145–154.
274. Marrink, S. J. and Lindahl, E. (1999) Cholesterol in lipid bilayers. *Biophys. J.* **77**:145–154.
275. Marrink, S. J. and Lindahl, E. (1999) Cholesterol in lipid bilayers. *Biophys. J.* **77**:145–154.
276. Marrink, S. J. and Lindahl, E. (1999) Cholesterol in lipid bilayers. *Biophys. J.* **77**:145–154.
277. Marrink, S. J. and Lindahl, E. (1999) Cholesterol in lipid bilayers. *Biophys. J.* **77**:145–154.
278. Marrink, S. J. and Lindahl, E. (1999) Cholesterol in lipid bilayers. *Biophys. J.* **77**:145–154.
279. Marrink, S. J. and Lindahl, E. (1999) Cholesterol in lipid bilayers. *Biophys. J.* **77**:145–154.
280. Marrink, S. J. and Lindahl, E. (1999) Ch

state and Mat. Sci. **1**:387–
stacles to success. *Science*
d DNA-transfection pro-
re of DNA-cationic lipi-
stinct interhelical packing
ensional smectic ordering
Phys. Rev. Lett. **79**:2582–
of a rectangular columnar
et al. **81**:5015–5018.
pic structural changes of
A complexes compared to
erted hexagonal phase of
science **281**:78–81.
bled cationic lipid–DNA
NA-lipid complex. *Phys.*
ensional smectics interca-
-complexes. *Phys. Rev. Lett.*
e, stability, and thermo-
electric instability. *Euro.*
liposomes. *Biophys. J.*
352.
neum lipid models: fatty
: A molecular-dynamics
the structures of dimyris-
olecular dynamics simu-
Behavior of cholesterol
olecular-dynamics study.
olecular dynamics investi-
Biophys. J. **75**:2147–2156.
nosphatidylcholine/chol-
nics simulation. *Biophys.*
Cholesterol effects on the
Biophys. J. **78**:1376–1389.
and molecular dynamics
concentration. *Biophys. J.*

Dynamic Simulations of Biological Membranes

125. Brown, D. A. and London, E. (1998) Structure and origin ordered lipid domains in biological membranes. *Membrane Biol.* **164**:103–114.
126. Simons, K. and Ikonen, E. (1997) Functional rafts in cell membranes. *Nature* **387**:569–572.
127. Marrink, S. J. and Mark, A. E. (2001) Molecular dynamics simulations of mixed micelles modeling human bile. *Biochemistry* (2002) (in press).
128. Hristova, K., Dempsey, C. E., and White, S. H. (2001) Structure, location, and lipid perturbations of melittin at the membrane interface. *Biophys. J.* **80**:801–811.
129. Huang, H. W. (2000) Action of antimicrobial peptides: Two-state model. *Biochemistry* **39**:8347–8352.
130. Popot, J.-L. and Engleman, D. M. (1990) Membrane protein folding and oligomerization: The two-stage model. *Biochemistry* **29**:4031–4037.
131. White, S. H. and Wimley, W. C. (1999) Membrane protein folding and stability: Physical principles. *Annu. Rev. Biophys. Biomol. Struct.* **28**:319–365.
132. Marrink, S. J., Lindahl, E., Edholm, O., and Mark, A. E. (2001) Simulation of the spontaneous aggregation of phospholipids into bilayers. *J. Am. Chem. Soc.* **123**:8638–8639.
133. Lindahl, E. and Edholm, O. (2000) Mesoscopic undulations and thickness fluctuations in lipid bilayers and molecular dynamics simulations. *Biophys. J.* **79**:426–433.
134. Shelley, J. C. et al. (2001) A coarse grain model for phospholipid simulations. *J. Phys. Chem. B* **105**:4464–4470. Shelley, J. C. et al. (2001) Simulations of phospholipids using a coarse grain model. *J. Phys. Chem. B* **105**:9785–9792.
135. Goetz, R., Gompper, G. and Lipowsky, R. (1989) Mobility and elasticity of self-assembled membranes. *Phys. Rev. Lett.* **62**:221–224.
136. Marrink, S. J. and Mark, A. E. (2001) Effect of undulations on surface tension in simulated bilayers. *J. Phys. Chem. B* **105**:6122–6127.
137. Lindahl, E. and Edholm, O. (2000) Spatial and energetic-entropic decomposition of surface tension in lipid bilayers from molecular dynamics simulations. *J. Chem. Phys.* **113**:3882–3893.
138. Nagle, J. F. and Tristram-Nagle, S. (2000) Structure of lipid bilayers. *Biochim. Biophys. Acta* **1469**:159–195.